AD-A084 132 HEBREW UNIV JERUSALEM (ISRAEL) DEPT OF PHYSICAL CHE--ETC F/G 7/4
VIB-ROTATIONAL ENERGY TRANSFER AND RELAXATION PATTERNS IN NON-E--ETC(U)
MAR 80 A BEN-SHAUL AFOSR-77-3443
UNCLASSIFIED EOARD-TR-80-9 NL

1 OF 1
AD
A084132

END
DATE
FILMED
6-80
DTIC

(2)

LEVEL II

ADA084132

(19) REPORT DOCUMENTATION PAGE	READ INSTRUCTIONS BEFORE COMPLETING FORM
(18) ~~1. Report Number~~ EOARD-TR-80-9	2. Govt Accession No. AD-A084132
3. Recipient's Catalog Number	
4. Title (and Subtitle) (6) VIB-ROTATIONAL ENERGY TRANSFER AND RELAXATION PATTERNS IN NON-EQUILIBRIUM CHEMICAL SYSTEMS	5. Type of Report & Period Covered (9) Final [redacted] rept. 15 Sep [redacted]77 - 14 Sep [redacted]79
	~~6. Performing Org. Report Number~~
7. Author(s) (10) A. Ben-Shaul	8. Contract or Grant Number (15) AFOSR-77-3443
9. Performing Organization Name and Address The Hebrew University of Jerusalem Department of Physical Chemistry Givat-Ram, Jerusalem, Israel	10. Program Element, Project, Task Area & Work Unit Numbers (16) 23[redacted] (17) D1
11. Controlling Office Name and Address European Office of Aerospace Research and Development/LNC Box 14 FPO New York 09510	12. Report Date (11) Mar[redacted]80
	13. Number of Pages 72
14. Monitoring Agency Name and Address (12) 77p	15.
16. & 17. Distribution Statement Approved for public release; distribution unlimited.	
18. Supplementary Notes	

DTIC
ELECTE
MAY 13 1980
S D
E

19. Key Words

INTERNAL EXCITATION OF REAGENTS	THERMODYNAMIC CONSTRAINTS	ANHARMONIC EFFECTS
CHEMICAL AND MOLECULAR LASERS	ROTATIONAL RELAXATION	MAXIMAL WORK
V-V AND V-T RATE CONSTANTS	VIBRATIONAL RELAXATION	

20. Abstract

The characteristics of vibrational relaxation of diatomic molecules are analyzed using a combined kinetic-thermodynamic approach based on the master equation formalism on the one hand and the maximal entropy procedure on the other. The complex and detailed solutions for the vibrational relaxation of diatomic molecules (HF as a specific systen) can be greatly compacted and systemized. The physical-mathematical significance of detailed balancing and quasi-equilibrium distributions in non-isothermal systems are discussed. It is shown that the increased efficiency of rotationally relaxed chemical lasers is due to the removal of thermodynamic constraints from the molecular distribution function. The different roles of reagent internal excitation on the rates of endoergic reactions at a given temperature and a given total energy are discussed and demonstrated.

FORM 1473

80 5 12 139

DDC FILE COPY

163 155

This report has been reviewed by the Information Office (EOARD/CMI) and is releasable to the National Technical Information Service (NTIS). At NTIS it will be releasable to the general public, including foreign nations.

This technical report has been reviewed and is approved for publication.

John T Milton
JOHN T. MILTON
Scientific and Technical
Information Officer

Charles J LaBlonde
CHARLES J. LABLONDE
Lt Colonel, USAF
Director, Aeronautical Systems

FOR THE COMMANDER

Gordon L. Hermann
GORDON L. HERMANN
Lt Colonel, USAF
Executive Officer

Accession For
NTIS GRA&I ☒
DDC TAB ☐
Unannounced ☐
Justification

By
Distribution/
Availability Codes

Dist.	Avail and/or special
A	

Contract/ Grant Number: AFOSR 77-3443 (Modification No. 77-3443A)

VIB-ROTATIONAL ENERGY TRANSFER AND RELAXATION PATTERNS IN NONEQUILIBRIUM CHEMICAL SYSTEMS

A. Ben-Shaul
Department of Physical Chemistry
The Hebrew University of Jerusalem
Jerusalem, Israel

March, 1980

Final Scientific Report for the period Sept. 15, 1977 - Sept. 14, 1979.

Approved for public release;
distribution unlimited

Prepared for The United States Air Force

The Air Force Office of Scientific Research

and

EUROPEAN OFFICE OF AEROSPACE RESEARCH AND DEVELOPMENT
London, England

1. Introduction

This report reviews the results achieved during the two years (77 Sept. 15 - 79 Sept. 14) of the research project 'Vib-rotational energy transfer and relaxation patterns in nonequilibrium chemical systems', supported by the U.S. Air Force, via EOARD, as a low-cost ($ 4300 total) grant: AFOSR 77-3443 (modification No. AFOSR 77-3443A).

The report is divided into two parts: A) A survey of the objectives, results and conclusions of studies performed in the framework of the grant and published in the scientific literature. B) An appendix, containing copies of the relevant publications.

Much of the work carried out under the present project was done in collaboration with Professor R.D. Levine, in accordance with the proposals submitted. Some of the joint studies are summarized in the reprints of the articles included in Part B, (the appendix). Many other topics, directly and indirectly related to the present research grants, are discussed in a book entitled 'Lasers and Chemical Change', (Ref. 1), scheduled to appear in 1980. A copy of the Table of Contents and the *preface of this book* are also included in the appendix.

An interim scientific report covering the progress achieved during the first eighteen months of the grants has been submitted in March 1979. Consequently, there is a large degree of overlap between this, final, report and the interim report.

A. SURVEY

Contents: 1. Abstract

2. Background

3. Vibrational relaxation of diatomic molecules

4. Master equation for non-isothermal systems

5. Kinetic schemes, constraints and maximal work in chemical lasers

6. The rate of reagent internal excitation in chemical reactions.

7. Other topics

1. Abstract

The general purpose of the project was to provide new insights into the kinetics and thermodynamics of chemical systems far from equilibrium. The theoretical approaches adopted combine detailed kinetic analyses based on master equation solutions and thermodynamic algorithms aiming to reduce the intrinsic complexity of the detailed kinetics. The systems and problems addressed are of interest for chemical laser and laser induced chemistry studies. In one work we have analyzed the kinetic and thermodynamic aspects of V-V and V-T relaxation of HF molecules (Sec. 3). Another study deals with the formal and physical implications of master equations for non-isothermal relaxation, in particular the significance of detailed balance and quasi-equilibrium distribution in some systems (Sec. 4). The thermodynamic origin for the enhanced efficiency of chemical lasers at rotational equilibrium is outlined in Sec. 5. The very different

effects of reagent internal excitation on the rates of endoergic reactions taking place at a given total energy and a given temperature were presented in an article summarized briefly in Sec. 6. Sec. 7 mentions some other topics, directly and indirectly, related and supported by the present grant.

2. Background

A prerequisite for selective chemical processes is the establishment of non-equilibrium populations. For example, one of the rapidly developing techniques for selecting a given chemical species from a chemical mixture involves laser excitation of this species to some excited state from which it can rapidly react with a given molecule to generate a product which in turn can be easily separated from the mixture. Another example, laser action requires very specific level populations, namely population inversion. In chemical lasers population inversion is achieved by means of an exoergic chemical reaction, e.g.

$$F + H_2 \rightarrow HF(v,J) + H \qquad (1)$$

which produces vib-rotationally excited diatomic molecules, (HF).

The relaxation process which begins immediately upon the establishment of nonequilibrium tends to carry the system back to equilibrium, thereby competing with the selective mechanism (e.g. the lasing process). Understanding the mechanisms and the time scales associated with relaxation processes is thus crucial for assessing the possibilities of selective-specific processes in chemical systems. This provides the major motivation for the studies carried out in the framework of the present research project. More specifically, we have been studying several aspects of vibrational and rotational relaxation of small molecules in the gas phase, as well as the effects of vib-rotational excitation on the rates of chemical reactions.

The most common tool for describing relaxation processes are the master equations governing the time evolution of the relaxing level populations. To solve these equations for realistic systems, one usually needs a multitude of rate coefficients whose exact experimental values are only rarely and partially available. In order to solve the master equations for HF molecules we have used the information theoretic synthesis method in order to determine the missing rate constants (for a review, see [2]). The thermodynamic-information theoretic approach has been applied not only to microscopic problems (analysis and synthesis of rate constants for detailed processes), but also to the macroscopic characterization of the relaxation process. The key idea here is to identify the (usually very small) number of informative macroscopic varaibles which govern the time evolution of the system. Examples for such variables are the average number of vibrational quanta and the average energy per molecule. The latter is the only informative variable which survives after equilibrium has been achieved. The molecular distribution functions are found by maximizing the entropy of the system subject to the constraints implied by the momentary values of the macroscopic observables.

The kinetic and thermodynamic points of view are intimately related to each other, in all the topics studied in the framework of the project. The significance of these relations as well as their implications are described briefly below and in more detail in the enclosed manuscripts (part B).

3. Vibrational relaxation of diatomic molecules

In this section we outline the background and the results of ref. 3. We have chosen pure HF gas as a model system. The relaxation processes taking place in this system are traditionally divided into two classes: 1) V-V processes,

$$HF(n) + HF(m) \rightleftarrows HF(n') + HF(m'),\ n' + m' = n+m \qquad (2)$$

These processes conserve the number of vibrational quanta

$$\langle n\rangle = \Sigma P(n)n \qquad (3)$$

where P(n) is the vibrational distribution function. 2) V-T processes,

$$HF(n) + HF(m) \rightleftarrows HF(n') + HF(m'),\quad n' + m' \neq n+m \qquad (4)$$

which do not conserve $\langle n\rangle$.

The near resonant V-V processes are much faster than the V-T processes in the low energy regime (small n,m). Due to the vibrational anharmonicity the V-T processes are the dominant ones in the high energy regime [1-4]. Due to the anharmonicity, the fast V-V processes tend to establish a partly inverted (Treanor) quasi-equilibrium vibrational distribution in the low n region, which persists over a short time scale $\tau \sim \tau_{VV} << \tau_{VT}$. (The 'Treanor up-pumping' process is an important pumping mechanism in electrical and chemical CO lasers). At later times, $t \sim \tau_{VT}$, the V-T processes take over and restore the system to equilibrium.

In order to examine the above notions in a quantitative fashion we have first solved the vibrational master equation, using a comprehensive set of over 300 rate coefficients [1-4]. We have then employed the maximal entropy procedure in order to identify the thermodynamic constraints describing the relaxing populations. The two major concrete findings were: a. In most cases two constraints, the average number of quanta, <n>, and the average vibrational energy $\langle E_n \rangle = \Sigma P_n E_n$ suffice to characterize the relaxation. b. During the first, V-V dominated stage, the vibrational populations can be described as a superposition of the initial and a quasi-equilibrium vibrational distribution (common to all conditions or, equivalently, independent of the initial distribution). Another, more general result provided in ref. 3 is a proof of the existence of a generalized thermodynamic potential characterizing the relaxation - independently of the molecularity of the collision microscopic mechanism which causes the relaxation.

4. Master equations for non-isothermal systems

This study has been summarized in a short note, ref. 5. The motivation for this work has been in a misleading procedure (in our opinion) suggested in ref. 4, to determine the stationary solutions of the master equation The suggestion is to substitute a postulated solution into the equation and check the consistency. We argue that this procedure can be harmful since the stationary solutions have to satisfy not only the master equation itself, but also the appropriate boundary conditions. In non-isothermal systems these conditions are not trivial and must be carefully formulated. As a result of these notions, we have proposed a general, consistent, algorithm which removes the possibility of misconceptions and misidentifications of the stationary solutions. The key idea is to start with the full master equations for all the time dependent degrees of freedom in the system. Then, the true stationary solutions are found by detailed balance relations involving the maximal entropy distributions for all degrees of freedom. Reduction of the master equation by separating the relaxation processes into different time scales can then be applied without violating the boundary conditions and without altering the physical significance of quasi-equilibrium distributions and momentary detailed balance relations.

5. Kinetic schemes, constraints and maximal work in chemical lasers

It is known experimentally that the efficiency of chemical lasers is significantly increased by adding a buffer gas to the lasing mixture. The gas moderates temperature rise and ensures fast rotational relaxation. The latter phenomena enables more efficient extraction of laser radiation from partially inverted vibrational populations. Kinetic considerations can be used to set upper bounds to the efficiency of the laser in the limits of fast and slow rotational relaxation [6]. In ref. 7 we have provided complementary thermodynamic interpretations. To this end we have proved several general results concerning the maximal work that can be extracted from a nonequilibrium chemical system. In particular, it was shown that the lower is the number of constraints on the molecular distribution function the higher is the efficiency of converting internal energy into thermodynamic work. We have applied this result to chemical lasers in which the thermodynamic work appears as coherent laser radiation[1,6].It was shown explicitly that in the limit of weak rotational coupling (slow rotational relaxation) the molecular distribution function is subjected to many constraints. These are removed in the strong coupling limit. This explains the higher efficiency at rotational equilibrium.

6. The role of reagent internal excitation in chemical reactions

Internal excitation of translationally thermal reagents leads usually to dramatic enhacements of the rates of endoergic reactions. This is primarily a thermodynamic (statistical) effect since internal excitation reduces the endoergicity of the reaction. On the other hand, the effect of raising the internal energy at a given total collision energy (implying a reduction in the translational energy) is purely dynamical. In fact, internal excitation under such conditions does not necessarily lead to enhancement of the rate, and only when the reversed (exothermic) reaction results with population inversion enhancement by one or two orders of magnitude are expected. The different roles of reagent internal excitation at given energy and given temperature are of theoretical as well as practical importance and must be taken into account in analyzing experimental data. The origin and significance of these differences are discussed in ref. 8.

7. Other topics

The book cited as ref. 1 includes various topics directly and indirectly related to the present research projects which have not, or only partly, been published elsewhere. We (R.D. Levine and A. Ben-Shaul) acknowledge our AFOSR grants which helped understanding, clarifying and presenting these issues. It will be impossible as well as redundant to outline the relevant problems in this report and it should therefore be sufficient to just name a few, viz.: Rotational relaxation of diatomic molecules; the connection between vibrational and rotational relaxation of diatomic molecules; kinetic and thermodynamic aspects of the relaxation characteristics of laser excited polyatomic molecules.

References

[1] A. Ben-Shaul, Y. Haas, K.L. Kompa and R.D. Levine, 'Lasers and Chemical Change', Vol. 10 in Springer Series in Chemical Physics (Springer Verlag, Heidelberg, 1980).

[2] R.D. Levine and A. Ben-Shaul, Chap. 4 in 'Chemical and Biochemical Applications of Lasers', C.B. Moore ed. (Academic Press, New York, 1977).

[3] M. Tabor, R.D. Levine, A. Ben-Shaul and J.I. Steinfeld, Mol. Phys. 37, 141 (1979).

[4] C.E. Treanor, J.W. Rich and R.G. Rehm, J. Chem. Phys. 48, 1798 (1968).

[5] A. Ben-Shaul and M. Tabor, Chem. Phys. Lett. 61, 571 (1979).

[6] A. Ben-Shaul in 'Photoselective Chemistry' (A special issue of Advances in Chemical Physics), J. Jortner, R.D. Levine and S.A. Rice eds. (Wiley, New York, 1980).

[7] A. Ben-Shaul and R.D. Levine, J. Noneq. Ther. 4, 363 (1979).

[8] A. Ben-Shaul and R.D. Levine (submitted to Chem. Phys. Letts.)

J. Non-Equilib. Thermodyn.
Vol. 4 (1979), pages 363–376

Molecular Constraints Implied by Kinetic Coupling Schemes and Maximal Work in Chemical Lasers

A. Ben-Shaul, R. D. Levine
Dept. of Physical Chemistry and Institute for Advanced Studies, The Hebrew University, Jerusalem, Israel

Received 4 December 1978
Registration Number 114
Key Number 26 02 225

Abstract

The efficiency of molecular lasers is known to be enhanced when certain relaxation processes (which dissipate some energy) are allowed to take place. We consider a thermodynamic interpretation of such observations with special applications to chemical lasers operating in the limits of slow and fast rotational relaxation. Specifically it is shown that kinetic coupling schemes which reflect the hierarchy of rate processes in a nonequilibrium molecular system can be expressed as thermodynamic constraints on the internal state distribution function. The lower the number of constraints the higher is the work which can be extracted from the nonequilibrium populations. The lower laser efficiency in the absence of rotational relaxation is due to the existence of an isolating constraint on the vib-rotational populations of the lasing molecules.

Introduction

Experiments [1, 2] and numerical simulations [3] show that the efficiency of a chemical laser is significantly enhanced in the presence of a buffer gas. A kinetic interpretation [4] (the 'funnel effect' [1], see below) invoking a competition between stimulated emission and the (pressure dependent) rotational relaxation is available. The purpose of this paper is to offer a corresponding thermodynamic interpretation. The discussion illustrates the general approach to systems in molecular disequilibrium [5, 6] which is based on the maximal entropy formalism [7]. The increase of the laser efficiency with the buffer gas pressure is shown to reflect the additional work which is available from a system when a constraint is removed.

The constraints which are introduced in the discussion of thermodynamic work processes [8–10] are typically macroscopic (e. g. pistons, catalysts). A novel feature of the present discussion is that work is obtained by the removal of a molecular (i. e. a kinetic or mechanistic) constraint. Specifically, the constraints to be discussed are conditions on the distribution of the molecules over their internal energy levels.

0340-0204/79/0363-0376$02.00
© Copyright by Walter de Gruyter & Co. · Berlin · New York

In a laser system the work is extracted as light which due to its spectral characteristics (well collimated beam over a very narrow frequency range) can be regarded as thermodynamic work [11].

Section 1 is a discussion of the work available upon (partial) removal of the constraints on the system. The maximal entropy formalism enables us to introduce the molecular constraints in a simple fashion and to demonstrate their role not only analytically but also in a graphic fashion. A particular feature of the discussion is that it is not limited to systems coupled to a heat bath [12]. The particular constraints which are removed due to the presence of a buffer gas are formulated in section 2, which applies the point of view of section 1 to the physical system of interest.

On the microscopic level we are concerned with the following physical picture. A fast chemical reaction creates a disequilibrium population of molecules in their vibrational and rotational states. In the low pressure regime lasing is possible on any allowed[1] molecular line for which there is an excess population in the upper state. Laser emission depletes the upper state and hence terminates when the populations in the upper and lower state become equal (or, in practice, when the excess in the upper state falls below the threshold density required by losses etc [2, 4]). Collisional processes (whose rate is proportional to the pressure) are too slow as compared to the rate of laser emission in order to drain the upper state or to feed the lower state. The entire system acts as a collection of independent two-level systems. For each molecular laser line the sum of the populations in the upper and lower states is constant (on the time scale of interest).

As the pressure is increased, collisional relaxation begins to take place. The critical observation here is that rotational energy transfer is several orders of magnitude *more effecient than vibrational* energy transfer [1, 13]. Hence rotational relaxation can but vibrational relaxation typically cannot compete with the (unimolecular) lasing process [1]. In the limit where rotational energy transfer is quite efficient any depletion of an upper state due to lasing[2] is immediately restored by the collisional process and any excess of the lower state is immediately removed. The net result of this "cooperative" lasing mechanism is an efficient draining of the population of the upper vibrational state into the lower one.

The low pressure constraint that on any lasing line the total population (sum of upper and lower states) must be constant is thus removed in the higher pressure regime.

In the limit of strong rotational coupling the rotational distribution is thermalised throughout the lasing. Thus,

$$P(v, J) = P(v)\,(2J + 1)\exp[-\beta B J(J + 1)]/Q_{rot}(\beta)\,. \qquad (1)$$

---

[1] Dipole selection rules limit the allowed transitions. In lasers using diatomic molecules the important transitions occur on the P-branch lines connecting the vibrotational levels, $(v, J - 1)$ to $(v - 1, J)$. Here v and J are the vibrational and the angular quantum number respectively.

[2] It is important to note that lasing occurs on the strongest ('Highest gain' [1, 2]) line. During the lasing process, this line gradually shifts towards higher J's, see below.

where $T = (R\beta)^{-1}$ is equal to the translational temperature. For simplicity we have used here the rigid rotor level scheme and B is the rotational constant. The necessary lasing condition, i. e. population inversion,[3]

$$P(v, J-1)/(2J-1) > P(v-1, J)/(2J+1)\,, \tag{2}$$

now reads

$$J > (2\beta B)^{-1}\,\ell n[P(v-1)/P(v)]\,. \tag{3}$$

Lasing starts on the line with the highest inversion (more precisely highest gain) corresponding to the initial population P(v). Generally this is one of the low lying J's. The fast rotational relaxation transfers molecules into v, J − 1 and from v − 1, J while preserving the Boltzmann shape of the rotational distributions and preventing "hole burning". The upper vibrational population is thus homogeneously drained (funnelled [1]) into the lower one through the highest gain transition. As P(v − 1)/P(v) increases in this process the lasing is gradually shifted to higher J's as implied by (3). Since J is unlimited, lasing can still go on even when $P(v-1)/P(v) \ll 1$. In practice, lasing terminates at some high J determined by the requirement for threshold inversion [2, 4]. Yet the draining of the upper level due to the cooperation (strong coupling) between the rotational levels is very efficient.

In the low pressure region collisional relaxation is negligible and the population P(v, J) is affected only by the stimulated emission. Thus, molecules can be exchanged only between (v, J − 1) and (v − 1, J) and the different lines form distinct groups. Here the lasing terminates when every line reaches, individually, an equality in (2) so that lasing terminates when $P(v)/P(v-1) \sim 1$; as opposed to the strong coupling case. The passage to the strong coupling limit is formally achieved by removing the constraints on population exchange between the different rotational states of the same vibrational manifold.

1. Work

Discussion of work processes for systems in disequilibrium is conveniently formulated using the maximal entropy formalism [5, 6, 12]. Our first purpose is to relate this point of view to the "energy picture" [8], which is more common in equilibrium thermodynamics. In doing so we shall also introduce our notation and invoke the distinction between the allowed and excluded regions in the mean or internal energy E-entropy S plane which is fundamental to our subsequent discussion.

Our primary concern is with systems in internal molecular disequilibrium where upon spontaneous removal of the constraints the relaxation towards equilibrium is predominately collisional. We shall thus assume that the system is spatially homogenous, dilute and that the time scale of interest is sufficiently coarse that collisions are instantaneous. A complete microscopic characterisation of the system is then provided by the number of molecules in each of the different internal energy states. One can thus consider a distribution function P(n, t) specifying the fraction of all molecules in the internal energy level n (of degeneracy g_n) at the time t.

---

[3] P(v, J − 1) is the population in the 2(J − 1) + 1 = 2J − 1 fold degenerate (v, J − 1) vibrotational level. The population per quantum state is P(v, J − 1)/(2J − 1). Population inversion requires inversion between quantum states, [2].

A macroscopic characterisation of the state of the system is provided by specifying the value of m "constraints"

$$\langle A_r \rangle = \sum_n A_r(n)\, P(n, t)\,, \qquad r = 1, \ldots, m\,, \tag{4}$$

which together with the normalisation

$$1 = \langle A_0 \rangle = \sum_n P(n, t)\,, \tag{5}$$

suffice to determine P(n, t). In (4), $A_r(n)$ is the magnitude of the property A_r in the n'th level. Unless n is comparable to the number of levels which are significantly populated, the m + 1 constraints, (4) and (5) do not suffice, in themselves, to specify a unique distribution function P(n, t). It is here that one invokes the principle of maximum entropy [6] by selecting P(n, t) as that distribution which satisfies the m + 1 constraints and whose entropy[4]

$$S[n] = -R \sum_n P(n, t)\, \ln[P(n, t)/g_n] \tag{6}$$

is maximal. Provided that the (m + 1) constraints are linearly independent and that their values are consistent (i. e. there is at least one distribution which satisfies (4) and (5)) the maximum problem has a unique solution [14]. Another important feature of the solution is that the addition of constraints can never cause the entropy to increase. Intuitively this is obvious. Adding constraints can only further restrict the range of contending distributions and hence the entopy will at most not change[5] and otherwise will decline. Finally, one notes that the entropy is a convex function of the constraints [14], i. e. for any P(n, t) that satisfies the m + 1 constraint conditions we have

$$\partial^2 S[n]/\partial \langle A_r \rangle^2 < 0\,, \tag{7}$$

where the inequality is strict when the constraints are linearly independent.

The three properties of the maximum entropy procedure are summarised graphically in the top row of Figure 1 where E is the mean energy (per mole) of the system

$$E = \sum_n E_n P(n, t)\,. \tag{8}$$

---

[4] Equation (6) is the entropy for one mole. Since, by assumption, the gas is dilute and the collisions are uncorrelated, the single molecule distribution function sufficies to describe the system. However, the system consists of N molecules rather than of a single one.

[5] This happens when the additional constraint is "non-informative" [6, 15], i. e. when it does not help to specify the macroscopic state.

Given the value of E, there is a unique maximal value of S shown as the solid line. Moreover, the solid line is convex (cp. (7)). Finally, if additional constraints are present then, for a given value of E, the value of S can only go down. In the S-E plane, the solid line is the boundary between the allowed and excluded states of the system. A given (S, E) point can only be on or below the solid line. It is not possible to find a macroscopic state which is subject to the constraints whose entropy exceeds the boundary line. The physical significance of this boundary is made clear by equilibrium thermodynamics. The normalised distribution of maximal entropy subject only to a given value of the energy is, of course, the equilibrium ('canonical') thermal distribution. The slope of the S-E curve is then a measure of the temperature[6]

$$\partial S/\partial E = 1/T = R\beta \,, \tag{9}$$

and the condition that the distribution be normalised determines the partition function

$$Q = \sum_n g_n \exp(-\beta E_n) \,. \tag{10}$$

The sum over levels in (10) may converge even if β is negative (e. g. if there are only a finite number of levels), in which case the S-E curve can have a maximum (upper left case in Fig. 1). If the sum (10) converges only for positive β (e. g. if the spectrum is unbounded from above) then the S-E curve is monotonic (upper right case in Fig. 1).

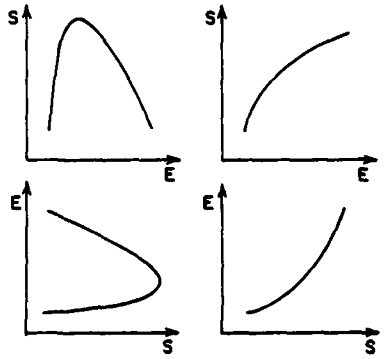

Fig. 1: Maximal entropy curves in the entropy S (upper row) and mean or internal energy E (bottom row) representations for systems with bounded (left column) and unbounded (right column) spectrum. In the S representation every E, S point on the solid curve is obtained by maximizing S subject to the value of E while in the E representation every E, S point on the curve corresponds to the extremal E for a given S (where for the negative temperature region, $R\beta = \partial S/\partial E < 0$, of systems with bounded spectrum, the extremum is a maximum). The allowed region of nonequilibrium E, S points lies on the concave side of the solid curves.

---

[6] We use the term temperature in a generalized sense as the (inverse) magnitude of the Lagrange parameter (cp. (11)) conjugate to the energy. The letter k denotes Boltzmann's constant.

An alternative macroscopic description and one that is well suited towards the discussion of work processes in an isolated system regards the energy E as a function of the entropy S and other macroscopic variables. This is sometimes known as "the energy picture" [8]. We now show that the tranformation from the entropy to the energy picture is not limited to systems in thermal equilibrium but can be carried out in general.

Assume the energy to be taken as the first (i. e. $r = 1$) constraint. The problem of seeking an extremum of the entropy subject to $m + 1$ constraints can be formulated as seeking the unconstrained extremum of the Lagrangian

$$L = S[n] - (\lambda_0 - 1)\langle 1\rangle - R\beta E - \sum_{r=2}^{m} \lambda_r \langle A_r\rangle . \qquad (11)$$

Here the $m + 1$ coefficients ($\lambda_0, \beta, \lambda_r; r = 2, \ldots, m$) are parameters whose values are to be determined by the condition that at the extremum the distribution is consistent with the values of the constraints. One can show that the procedure leads not only to an extremum but indeed to a maximum for the entropy [6, 14]. Say now that L is divided by $R\beta$. The result (cp. (11)) is just a Lagrangian for seeking an extremum of the energy subject to the given value of the entropy and the other m constraints (normalisation and $\langle A_r\rangle$, $r = 2, \ldots, m$). This is the characterisation of the macroscopic state in the energy picture. The only difference is that the extremum is not necessarily a minimum. It will be a *minimum* if (as is typically the case for macroscopic systems) $\beta > 0$. It is a *maximum* if $\beta < 0$.

The formal equivalence between the entropy and the energy pictures is also shown in Fig. 1. The E-S plots in the bottom row are obtained by simple rotation from those in the top row. As in the entropy picture, the line is the boundary between the allowed and excluded macroscopic states. When $\beta > 0$, the equilibrium E-S line is concave.

Work processes in an isolated system are shown schematically in Figure 2. As in Figure 1 the solid E-S curve corresponds to the situation where no other constraints (apart from normalisation) are present. If additional constraints do apply, the system is characterised by some point (e. g. E_i, S_i) within the allowed region. If now some of these additional constraints are removed, part of the energy of the macroscopic state can be extracted as work. If the entropy is unchanged, then say E_j, S_i is a possible final macroscopic state. Removing additional constraints (at constant entropy) enables the energy to drop even further untill, when all constraints are removed, it reaches E_f. For the given value of S_i, $E_i - E_f$ is the maximal work that can be extracted from the system. If the entropy does increase, less work is available.

By regarding every allowed macroscopic state of the system as a state of maximal entropy subject to constraints one obtains a statistical mechanical description of work processes also for systems not in thermal equilibrium. (The corresponding thermodynamic description is well known [9, 10, 16]). Within such a formulation, equilibrium is the state where the constraints are the (additive) time-independent constants of the motion. There are however time-dependent constants of the

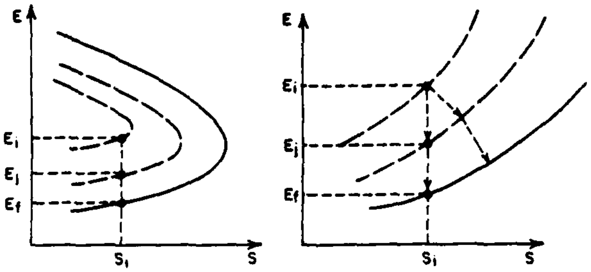

Fig. 2: Work processes in an isolated system of molecules with bounded (left) and unbounded (right) spectrum. The solid lines represent the equilibrium mean or internal energy E-entropy S locus. The broken lines are maximal entropy curves in the presence of additional constraints; the larger the number of constraints the lower is the value of S for a given E. Removal of constraints enables the system to convert part of its energy into work. In the regions of positive temperature, $\partial S/\partial E > 0$, the maximal work, e. g. $E_i - E_j$ is obtained in an isentropic process, $S_i = S_j$. Less work is available in an irreversible process $S_j > S_i$.

motion.[7] By maximizing the entropy subject to such constraints one obtains exact solutions of the Liouville equation which describe non-equilibrium situations. An *explicit construction principle* for such observables has been described, [17].

The graphical considerations of Fig. 2 can be cast in quantitative terms by recognizing that every point in the allowed region is determined as the solution of an extremum problem. Assume we vary the energy but keep all the other $\langle A_r \rangle$'s constant. For each energy we determine the maximal entropy. The locus of E-S pairs determined in this fashion is shown as a broken line in Fig. 2. (The solid line is, of course, a particular example of a broken line.) Now, let one or more constraints be dropped and the procedure repeated. This generates another broken line which is everywhere exterior to the previous broken line, (imagine Fig. 2 in the entropy picture). The solid line is exterior to all the broken lines.

Let $P_i(n)$ be the distribution of maximal entropy subject to the value E_i of the energy and to additional constraints. The distribution $P_j(n)$ (cp. Fig. 2) differs from $P_i(n)$ in that its energy is lower and some among the constraints on $P_i(n)$ are no longer operative for $P_j(n)$. However, by construction, all of the constraints on $P_j(n)$ are also valid for $P_i(n)$. In other words in going from i to j we have only removed[8] (but have not added) constraints.

As a distribution of maximal entropy $P_j(n)$ is necessarily of the functional form

$$P_j(n) = g_n \exp[-E(n)/RT^j - \sum_{r=2}^{m} \lambda_r^j A_r(n)]/Q_j \, . \qquad (12)$$

---

[7] These are observables which depend explicitly on time but whose average values are time-independent.

[8] It is important to note that the quantitative argument (eq. (13)) below requires that those constraints which remain do not change their value.

where only the constraints on the state j are present explicitly in the exponent in (12). Consider now the following transformations of the entropy deficiency [6, 12], $DS[P_i|P_j]$, where (12) is used in the final stage[9]

$$\begin{aligned} DS[P_i|P_j] &= R\sum_n P_i(n)\,\ell n[P_i(n)/P_j(n)] \\ &= R\sum_n P_i(n)\,\ell n[P_i(n)/g_n] \\ &\quad - R\sum_n P_j(n)\,\ell n[P_j(n)/g_n] \\ &\quad - R\sum_n [P_i(n)-P_j(n)]\,\ell n[P_j(n)/g_n] \\ &= S_j[n]-S_i[n] \\ &\quad + R\sum_n [P_i(n)-P_j(n)][\beta^j E(n)+\sum_r \lambda_r^j A_r(n)-\ell n Q_j] \\ &= S_j[n]-S_i[n]-R\beta^j\sum_n E(n)\,[P_j(n)-P_i(n)] \\ &= \Delta S-\Delta E/T^j\,. \end{aligned} \tag{13}$$

Only those constraints on $P_j(n)$ whose values for $P_j(n)$ and $P_i(n)$ are different appear in the final answer. Of course, this result follows from our initial stipulation that apart from the energy and the entropy, all other constraints on $P_j(n)$ are equally valid for $P_i(n)$. If, in addition $S_i[n]=S_j[n]$, we get

$$DS[P_i|P_j] = -\Delta E/T^j\,. \tag{14}$$

Since $-\Delta E$ is the maximal work available (Fig. 2) it follows that $T^j DS[P_i|P_j]$ is the maximal work even if the system is isolated and not coupled to a heat bath. Moreover, for the conditions in Fig. 2 we have

$$\begin{aligned} E_i-E_f &= (E_i-E_j)+(E_j-E_f) \\ &= T^f\,DS[P_i|P_f] \\ &= T^j\,DS[P_i|P_j]+T^f\,DS[P_j|P_f]\,. \end{aligned} \tag{15}$$

2. Lasing

In this section we explicitly introduce the constraints which are removed by collisional relaxation and consider the additional work made available by their removal. To simplify the algebra we shall assume that lasing occurs only on P-branch

---

[9] Since $DS \geq 0$, [6, 12], it follows that for a positive T, the maximal work is obtained when $\Delta S = 0$.

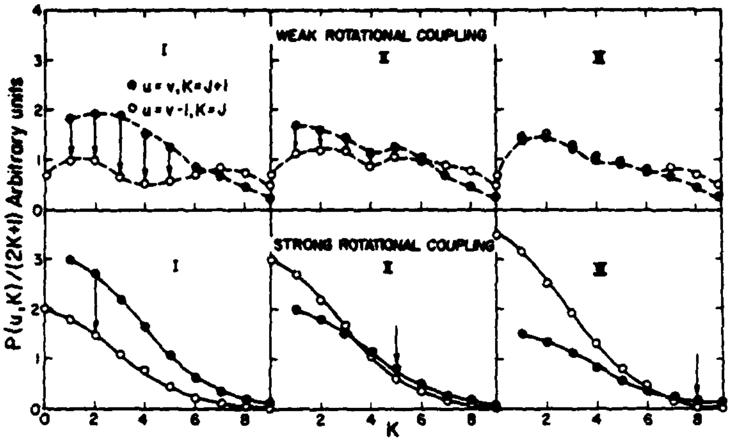

Fig. 3: Stages in the time evolution of the vib-rotational distribution function during the lasing process in the limits of slow (upper pannel) and fast (lower pannel) rotational relaxation. (I . . . just after *threshold*, II . . . *during* lasing, III . . . at the end of the pulse). In the limit of fast rotational relaxation the lasing line is an isolated subsystem; lasing occurs independently on each line and terminates upon equalization of the upper and lower populations. In the limit of fast rotational relaxation lasing occurs only on the highest gain line. The effective rotational energy transfer enables the system to lase on high J-lines thereby allowing a very efficient draining of the upper vibrational manifold and consequently high laser efficiency.

lines and that only two vibrational manifolds take part, as is shown in Fig. 3. (This is the case for example in the $Cl + HBr \rightarrow Br + HCl$ chemical laser [3]). Under such conditions one can easily establish a unique correspondence between the internal energy labels (v and J) of diatomic molecules and the possible lines in the P-branch $(v, J-1 \rightarrow v-1, J)$. Since the lasing is between only two vibrational manifolds, specifying the final rotational state J uniquely assigns the line. Specifying the vibrational quantum number v uniquely assigns the upper or lower state of the transition. Thus, while one often resolves the internal state distribution P(v, J) as

$$P(v, J) = P(J|v)\,P(v)\,, \tag{16}$$

i. e. a distribution of J states within a given vibrational manifold times the vibrational distribution, here we prefer the equivalent but complementary resolution

$$P(u, K) = P(u|K)\,P(K)\,. \tag{17}$$

In (17) we use the same convention as in Fig. 3,

$$P(K) = P(u, K-1) + P(u-1, K) \tag{18}$$

and

$$P(u|K) = \begin{matrix} P(v, K-1)/P(K) & u = v \\ P(v-1, K)/P(K) & u = v-1. \end{matrix} \tag{19}$$

P(K) is thus the sum of the population in both the upper and lower states of the given P-branch line and hence is the quantity that is constrained in the low pressure limit. P(K) can clearly (cp. (18)) be expressed as an average over the internal state distribution

$$P(K) = \langle A_K \rangle = \sum_v \sum_J A_K(v, J)\, P(v, J)\,, \tag{20}$$

$$\begin{aligned} A_K(v, J) &= \delta(v - u)\, \delta(J - K - 1) \\ &\quad + \delta(v - 1 - u)\, \delta(J - K)\,. \end{aligned} \tag{21}$$

The low pressure constraint is thus that the magnitude $\langle A_K \rangle$, K = 1, 2, . . . is specified to be equal to that value of P(K) which is characteristic of the nascent (i. e. strictly unrelaxed) products of the chemical reaction.

In Section 1 we have argued that removal of a constraint enables the system to perform work. The proof was based on the unique (and maximum) solution of the extremum entropy problem. Here one can identify explicitly the origin of the increase in the entropy due to the removal of the constraint. The reason is that the expression of the constraints $\langle A_K \rangle$ in the form (20) enables us to state that in the low pressure regime (and over the time interval of interest) the distribution P(K) is unchanging.

Corresponding to the resolution (17) one has a similar form for the degeneracy

$$\begin{aligned} g(u, K) \equiv g(v, J) &= 2J + 1 \\ &= g(u|K)\, g(K)\,, \end{aligned} \tag{22}$$

where $g(K) = [2(J - 1) + 1] + [2J + 1] = 4J$, so that

$$g(u|K) = \begin{cases} (2J - 1)/4J & u = v \\ (2J + 1)/4J & u = v - 1\,. \end{cases} \tag{23}$$

The entropy of the internal state distribution P(v, J) can thus be written as

$$\begin{aligned} S[v, J] &= -R \sum_{v,J} P(v, J)\, \ln[P(v, J)/(2J + 1)] \\ &= -R \sum_{K,u} P(u, K)\, \ln[P(u, K)/g(u, K)] \\ &= -R \sum_K P(K)\, \ln[P(K)/g(K)] \\ &\quad - R \sum_K P(K) \sum_u P(u|K)\, \ln[P(u|K)/g(u|K)] \\ &= S[K] + S[u|K] = S[u, K]\,. \end{aligned} \tag{24}$$

The first term in (24) is not allowed to vary in the low pressure regime. The procedure of seeking the distribution P(v, J) for which S[v, J] is maximal (subject to energy and other, if any, constraints) is equivalent to seeking the distribution P(u, K) for which S[u, K] is maximal (subject to the same constraints). In the low pressure regime P(K) = const. is a constraint, for all K's. As the pressure is increased, this constraint is removed (by collision induced population transfer). For a given E, the maximal value of S may be higher in the higher pressure regime since both P(u|K) and P(K) are allowed to vary. Conversely, for a given S, the minimal value of E will be lower (cp. Fig. 2) and more work is available.

Additional insight into the role of rotational energy transfer is provided by regarding the entire (isolated) system as a sum of two parts: the internal degrees of freedom of the lasing molecules and a heat bath provided by the translational motion. Coupling between the two is provided by binary collisions and hence is absent in the low pressure regime. In the limit of effective rotational relaxation the coupling is strong enough to ensure that at all times the rotational states are in thermal equilibrium at the temperature of the heat bath [18].

The coupling of the lasing system and heat bath implies that the entropy of the lasing system may decrease during lasing provided that there is a corresponding increase in the entropy of the bath [11, 19], Fig. 4. As is evident from the figure, the more the entropy of the lasing system can decrease the more work is available. A quantitative entropy balance for a chemical laser in the strong rotational coupling regime can be obtained as follows [19]: The rotational state population is maintained unchanged by the collision. The only change is thus in the vibrational state population P(v). Now in a v → v − 1 transition the relations hold:

$$\delta E = hc\omega\delta P\,, \tag{25}$$

$$\delta S = -R\ln[P(v)/P(v-1)]\,\delta P\,. \tag{26}$$

Here δP is the decrease in P(v) (and the increase in P(v − 1)) and ω is the vibration frequency. Consider now the P-branch transition v, J − 1 → v − 1, J. The laser light

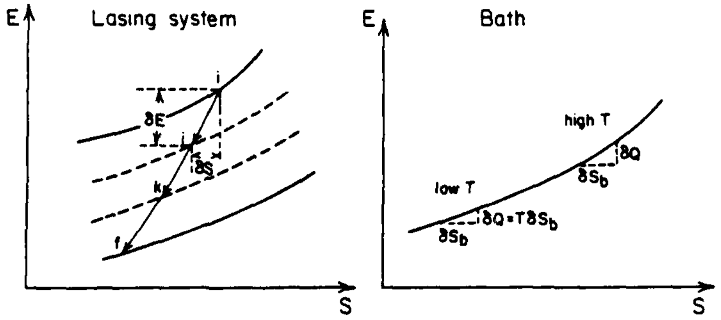

Fig. 4: Changes in the energy and entropy of the lasing system and the heat bath during lasing in the limit of strong rotational coupling. The entropy decrease of the system associated with lasing under partial vibrational inversion, $(P(v)/P(v-1) < 1)$, e. g. δS in the transition $i \rightarrow j$, is compensated for by a corresponding entropy increase of the bath $\delta S_b = \delta Q/T \geqslant -\delta S$. The difference $\delta W = -\delta E - \delta Q$ appears as laser radiation.

has a frequency $h\nu_L = h\omega - 2BJ$. The balance of the energy $(\delta E - h\nu_L)$ appears as heat in the bath. For this we have

$$\delta S_b = (2BJ/T)\,\delta P \tag{27}$$

where T is the temperature of the heat bath (Fig. 4). The condition

$$\delta S + \delta S_b \geqslant 0$$

or

$$2BJ/T + R\ell n[P(v)/P(v-1)] \geqslant 0 \tag{28}$$

is the familiar condition for chemical lasing [19], cp. (3).

Two additional insights are provided by (28). First note that even for $P(v)/P(v-1)$ quite below unity, lasing is still possible for a sufficiently high J. This is the reason for the gradual shift of the lasing line towards higher J's [1–3]. (Ultimately, lasing terminates due to the absolute concentrations falling below the loss level [4].) Second, the loss of chemical energy as heat is 2BJ. As the heat bath temperature increases, lasing occurs at a higher J (cp. (28)) and hence less energy is extracted as laser light. The efficiency improves upon cooling of the laser [1, 2].

3. Concluding remarks

The maximal work which can be obtained from a nonequilibrium molecular system has been discussed in terms of the number and character of the constraints on the molecular level populations. The constraints reflect the relative time scales of the relaxation and work producing processes governing the time evolution of the system. In chemical lasers based on vib-rotational transitions the major factor influencing the amount of work (laser light) which can be extracted from the system is the ratio between the rates of rotational relaxation and stimulated emission. When this ratio is large a constraint on the molecular distribution function is removed and the laser operates more efficiently.

It is important to note that all the considerations of this paper refer to the maximal and not the actual work obtained from nonequilibrium systems. The latter depends not only on the constraints but also on the rates of the loss processes which compete with the work producing mechanism. Thus, in chemical lasers vibrational relaxation and cavity losses compete with the stimulated emission and lead to irreversible entropy and heat production. However, time-dependent kinetic and thermodynamic analyses [20, 21] indicate that the major factors influencing the laser efficiency are the constraints implied by the kinetic scheme. Finally, it should be noted that the classification of rate processes as useful (e. g. rotational relaxation) and useless or dissipative (e. g. vibrational relaxation) depends on the form of thermodynamic work generated by the system. For example, while rotational relaxation enhances the stimulated emission in lasers operating on vibrational transitions it is, clearly, a process which should be avoided in lasers operating on pure rotational transitions.

Acknowledgement

Discussions on this work began in the workshop on "New Directions in Thermodynamics" held at the Aspen Center of Physics, Colorado in summer 1977. We would like to acknowledge the kind hospitality and stimulating atmosphere of the center. This work was supported by the Air Force Office of Scientific Research through its European Office, Grant no. AFOSR 77-3443A.

Bibliography

[1] Berry, M. J., Molecular Energy Transfer, Levine, R. D. and Jortner, J., Eds., p. 114 John Wiley and Sons, New York, 1976.
[2] Kompa, K. L., Chemical Lasers, Topics in Current Chemistry, vol. 37, Springer, Berlin, 1973.
[3] Keren, E., Gerber, R. B., Ben-Shaul, A., Computer Simulation of the Pulsed Cl + HBr Chemical Lasers: Effects of Rotational Non-Equilibrium, Chem. Phys., 21 (1976), 1.
[4] Ben-Shaul, A. Estimates of Chemical Laser Efficiencies in the Limits of Fast and Slow Rotational Relaxation, Chem. Phys., 18 (1976), 13.
[5] Levine, R. D., Entropy and Macroscopic Disequilibrium II, J. Chem. Phys., 65 (1976), 3302.
[6] Levine, R. D., Ben-Shaul, A., Thermodynamics of Molecular Disequilibrium, article in: Chemical and Biochemical Applications of Lasers, Moore, C. B., Ed., p. 145, Academic Press, New York, 1977.
[7] Levine, R. D., Tribus, M., Eds., The Maximum Entropy Formalism, MIT Press, Cambridge, 1978.
[8] Callen, H. B., Thermodynamics, Wiley, New York, 1961.
[9] Hatsopolous, G. H., Keenan, J. H., Principles of General Thermodynamics, Wiley, New York, 1965.
[10] Landau, L. D., Lifshits, E. M., Statistical Physics, Pergamon, Oxford, 1969.
[11] Levine, R. D., Kafri, O., Thermodynamic Efficiency of a Finite Gain Laser, Chem. Phys., 8 (1975), 426.
[12] Procaccia, I., Levine, R. D., Potential Work: A Statistical Mechanical Approach for Systems in Disequilibrium, J. Chem. Phys., 65 (1976), 3357.
[13] Levine, R. D., Bernstein, R. B., Molecular Reaction Dynamics, Oxford University Press, Oxford, 1974.
[14] Alhassid, Y., Agmon, N., Levine, R. D., An Upper Bound for the Entropy and Its Application to the Maximal Entropy Problem, Chem. Phys. Lett., 53 (1978), 22.
[15] Procaccia, I., Shimoni, Y., Levine, R. D., Entropy and Macroscopic Disequilibrium I., J. Chem. Phys., 65 (1976), 3284.
[16] Schottky, W., Ulich, H., Wagner, C., Thermodynamik, Springer, Berlin, 1929.
[17] Alhassid, Y., Levine, R. D., The Maximal Entropy Procedure as a Dynamical Theory, J. Chem. Phys., 67 (1977), 4321.
[18] Procaccia, I., Shimoni, Y., Levine, R. D., Rotational Relaxation: An Analytic Solution of the Master Equation with Application to HCl., J. Chem. Phys., 63 (1975), 3181.
[19] Levine, R. D., Kafri, O., Thermodynamic Analysis of Chemical Laser Systems., Chem. Phys. Lett., 27 (1974), 175.
[20] Ben-Shaul, A., Feliks, S., Kafri, O., Time Evolution of the Pulsed HF Chemical Laser. I. Kinetic Modelling-Rotational Nonequilibrium, Chem. Phys., 36 (1979), 291.
[21] Ben-Shaul, A., Kafri, O., Time Evolution of the Pulsed HF Chemical Laser II. Irreversible Thermodynamic Analysis, Chem. Phys., 36 (1979), 307.

Dr. A. Ben Shau
Professor Dr. R. D. Levine
Department of Physical Chemistry
The Institute for Advanced Studies
and Center for Energy Research
The Hebrew University
91000-Jerusalem, Israel.

MOLECULAR PHYSICS, 1979, VOL. 37, No. 1, 141–158

Microscopic and macroscopic analysis of non-linear master equations : vibrational relaxation of diatomic molecules

by M. TABOR†, R. D. LEVINE and A. BEN-SHAUL
Department of Physical Chemistry, The Hebrew University of Jerusalem, Jerusalem, Israel
and J. I. STEINFELD
Department of Chemistry, Massachusetts Institute of Technology, Cambridge, Mass. 02139, U.S.A.

(*Received* 6 *January* 1978)

The thermodynamic and kinetic characteristics of vibrational relaxation of diatomic molecules are studied using HF gas as a model system. The non-linear master equation governing the relaxation is solved numerically using a comprehensive set of exponential gap rate constants. The results indicate a two-stage relaxation mechanism. A very fast V–V dominated stage leading to an intermediate quasi-equilibrium distribution which depends only on the initial mean number of vibrational quanta. During this stage the vibrational distribution can be described as a superposition of the initial and intermediate distributions. A second, very slow, V–T dominated stage ultimately brings the system to complete equilibrium with the heat bath. The relaxation is characterized microscopically by the time evolution of the vibrational distribution and macroscopically by the evolution of the moments. The bridge between the two levels of analysis is provided by the *maximal* entropy procedure. It is shown that the entropy deficiency is the only convex function which decays monotonically to equilibrium irrespective of the order of the relaxation mechanism. Using the maximal entropy form of the distribution it is shown that two moments, i.e. two macroscopic observables, suffice to describe the distribution during the first stage while only a single moment is required to describe the final approach to equilibrium. During the intermediate stage more than two moments may be required.

1. INTRODUCTION

A relaxation process is characterized at the microscopic level by the time evolution of the population distribution. For a fairly wide class of problems this evolution is governed by linear master equations and in a number of special cases, e.g. harmonic oscillators coupled to a heat bath, it is even possible to obtain closed analytical solutions [1]. More generally though, exact solutions are not possible and one must resort to approximate schemes or numerical methods.

Recently the information theoretic characterization of (Markovian) relaxation processes has been discussed [2] and its use as a practical means of analysing such processes (when governed by a linear master equation) has been demonstrated [3]. The central idea is to use macroscopic properties of the system,

† Royal Society—Israel Academy Research Fellow.

i.e. bulk averages, provided they correspond to independent ('informative') observables, as constraints in a maximal entropy procedure to determine the relaxing population distribution. There are good reasons to justify the use of this procedure. For example, of the many convex functions that decay monotonically with the approach to equilibrium, and hence could be used to characterize the relaxation process, it is only the 'entropy deficiency' (its rate of decay is called the rate of entropy production) that satisfies essential 'additivity' or 'grouping' conditions [4, 5]. Further, it may be shown that, of all possible distributions consistent with the observed data, the maximal entropy distribution gives a lower bound for this rate [2]. Throughout this paper the term entropy refers exclusively to the information theoretic entropy (see [2–4]).

There are many processes, however, that are governed not by linear master equations but by *non*-linear master equations. These non-linear processes are of particular significance, for example, in molecular lasers. Here, fast vibrational–vibrational (V–V) transfer processes can, due to anharmonicity, cause rapid pumping up to inverted quasi-equilibrium distributions before the slower vibrational–translational (V–T) processes take over [6, 7]. Unfortunately, non-linear master equations are considerably less amenable to analytic investigation than their linear counterparts and can normally only be solved by approximation or numerical techniques. Obviously, then, alternative methods need to be investigated and, in view of its success for linear processes, the maximal entropy procedure is a likely candidate. Once again it is important to demonstrate the validity of such a procedure. In the next section we show that for non-linear master equations (unlike linear ones) the only convex function that has a definite rate of decay is the entropy deficiency. This result demonstrates that the entropy is a suitable, if not the only quantity with which to characterize the relaxation process. (Since the definite rate of entropy production can be interpreted as the generalized second law of thermodynamics, it seems eminently suitable to characterize the process with a quantity that satisfies this condition!)

In § 3 we give a detailed examination, with numerical examples, of the relaxation of a (dilute) gas of HF molecules. First we solve the relevant (non-linear) master equation numerically using a comprehensive set of exponential-gap [8, 9] state-to-state rate constants. These results illustrate general features of the process, e.g. effect of initial distribution, fast pumping to a quasi-equilibrium distribution and subsequent relaxation etc., as well as the time dependence of the moments (bulk observables). In § 4 we then go on to show how entropy provides a convenient characterization of the process and that the maximal entropy distribution, determined with only a small number of constraints, accurately reproduces (albeit phenomenologically at this stage) the evolving population distribution.

2. ENTROPY AND MACROSCOPIC DISEQUILIBRIUM

A linear master equation [1]

$$dP(n, t)/dt = \sum_m A(n, m)P(m, t)$$

specifies the time evolution of the population $P(n, t)$ in state n at time t. For convenience in later manipulations we rewrite it as a discrete equation over a short time interval Δt,

$$P(n, t+\Delta t) = \sum_m \Pi(n|m)P(m, t). \tag{2.1}$$

The $\Pi(n|m)$ give the probability that a system in state m will be found after Δt in state n. For Δt sufficiently small [1] $\Pi(n|m) = \delta_{n,m} + A(n, m)\Delta t$ and, in order to conserve probability

$$\sum_n \Pi(n|m) = 1. \tag{2.2}$$

The stationary distribution $P^0(n)$ is unchanged by the passage of time, i.e.

$$P^0(n) = \sum_m \Pi(n|m)P^0(m). \tag{2.3}$$

There are many functions of the form

$$E = \sum_n P^0(n)\phi\left[\frac{P(n, t)}{P^0(n)}\right], \tag{2.4}$$

which, for distributions governed by a linear master equation, satisfy $-dE/dt \geqslant 0$ provided only that the function $\phi = \phi(x)$ is convex (i.e. $\partial^2 \phi/\partial x^2 \geqslant 0$). This result is obtained in the form of the inequality [10]

$$\sum_n P^0(n)\phi\left[\frac{P(n, t)}{P^0(n)}\right] \geqslant \sum_n P^0(n)\phi\left[\frac{P(n, t+\Delta t)}{P^0(n)}\right], \tag{2.5}$$

by using the property that the mean of a convex function is greater than or equal to the function of the mean, i.e.

$$\langle \phi(x) \rangle_{\text{av}} \geqslant \phi(\langle x \rangle_{\text{av}}), \tag{2.6}$$

where the averaging is over any set of (normalized) probabilities. If the convex function is taken to be the entropy, i.e. $\phi(x) = x \ln x$, then (2.4) defines the entropy deficiency

$$\Delta S = \sum_n P^0(n)\frac{P(n, t)}{P^0(n)} \ln\left[\frac{P(n, t)}{P^0(n)}\right] = \sum_n P(n, t) \ln\left[\frac{P(n, t)}{P^0(n)}\right] \tag{2.7}$$

and its rate of change, the rate of entropy production, has a definite sign $-d\Delta S/dt \geqslant 0$. However, purely from this point of view, as mentioned in the introduction, there is nothing to distinguish our choice of the entropy as a means of characterizing the approach to equilibrium, from any other convex function. It is distinguished, though, by its additivity properties which, as we shall see, are of particular significance when we examine the evolution of functions of the form (2.4) for processes governed by *non-linear* master equations.

We write the stochastic equation for non-linear processes in the form

$$P(r, t+\Delta t) = \sum_{s, m, n} \Pi(rs|mn)P(m, t)P(n, t), \tag{2.8}$$

where the transition probabilities satisfy the conservation condition

$$\sum_{rs} \Pi(rs|mn) = 1. \tag{2.9}$$

The stationary distributions are defined in the same way as in equation (2.3), i.e.

$$P^0(r) = \sum_{s,m,n} \Pi(rs|mn)P^0(m)P^0(n). \tag{2.10}$$

Our aim is to see which functions of the form (2.4) still have a definite rate of decay. For this purpose it is convenient to reduce equation (2.8) by summing over one less index. This then gives a non-linear equation of the form

$$P(r, t+\Delta t)P(s, t+\Delta t) = \sum_{m,n} \Pi(rs|mn)P(m, t)P(n, t). \tag{2.11}$$

Notice that we write a product of distributions on both sides of the equation; this is to maintain its stochastic (or Markov) form and is consistent with its stationary form which must be

$$P^0(r)P^0(s) = \sum_{m,n} \Pi(r, s|mn)P^0(m)P^0(n). \tag{2.12}$$

We consider the convex function of the form

$$\phi = \phi\left[\frac{P(m, t)P(n, t)}{P^0(m)P^0(n)}\right] \tag{2.13}$$

and average it over the quantities $\Pi(rs|mn)P^0(m)P^0(n)/P^0(r)P^0(s)$ which, as can be seen from equation (2.12), can be regarded as a set of normalized probabilities, i.e.

$$\sum_{m,n} \Pi(rs|mn)\frac{P^0(m)P^0(n)}{P^0(r)P^0(s)} = 1. \tag{2.14}$$

Using the property of convex functions given in equation (2.6) we have

$$\sum_{m,n} \Pi(rs|mn)\frac{P^0(m)P^0(n)}{P^0(r)P^0(s)}\phi\left[\frac{P(m, t)P(n, t)}{P^0(m)P^0(n)}\right] \geqslant \phi\left[\sum_{m,n} \Pi(rs|mn)\frac{P(m, t)P(n, t)}{P^0(r)P^0(s)}\right], \tag{2.15}$$

which, by (2.8) becomes

$$\sum_{m,n} \Pi(rs|mn)P^0(m)P^0(n)\phi\left[\frac{P(m, t)P(n, t)}{P^0(m)P^0(n)}\right] \geqslant P^0(r)P^0(s)\phi\left[\frac{P(r, t+\Delta t)P(s, t+\Delta t)}{P^0(r)P^0(s)}\right], \tag{2.16}$$

summing over r and s and using the conservation condition (2.9) we obtain

$$\sum_{m,n} P^0(m)P^0(n)\phi\left[\frac{P(m, t)P(n, t)}{P^0(m)P^0(n)}\right] \geqslant \sum_{r,s} P^0(r)P^0(s)\phi\left[\frac{P(r, t+\Delta t)P(s, t+\Delta t)}{P^0(r)P^0(s)}\right]. \tag{2.17}$$

This is our basic result for a general convex function (of the form (2.4)) with distributions governed by a non-linear equation. This result can easily be generalized to processes of any order (molecularity). Thus for the stochastic equation of order s

$$P(n_1, t+\Delta t) = \sum_{\substack{n_2, \dots, n_s \\ m_1, \dots, m_s}} \Pi(n_1, n_2, \dots, n_s | m_1, m_2, \dots, m_s) \times \prod_{i=1}^{s} P(m_i, t), \tag{2.18}$$

we obtain the inequality

$$\sum_{n_1, \dots, n_s} \prod_{i=1}^{s} P^0(n_i)\phi\left[\prod_{i=1}^{s} \frac{P(n_i, t)}{P^0(n_i)}\right]$$
$$\geqslant \sum_{m_1, \dots, m_s} \prod_{i=1}^{s} P^0(m_i)\phi\left[\prod_{i=1}^{s} \frac{P(m_i, t+\Delta t)}{P^0(m_i)}\right]. \tag{2.19}$$

As it stands, our result is not very useful since it only relates products of distributions at earlier and later times. We do not obtain the simple result (2.5) that we have for linear processes. However, in the case of the entropy ($\phi(x) = x \ln x$) we can go further. Considering for simplicity the bimolecular process, equation (2.17) becomes

$$\sum_{m, n} P(m, t)P(n, t) \ln\left[\frac{P(m, t)P(n, t)}{P^0(m)P^0(n)}\right]$$
$$\geqslant \sum_{r, s} P(r, t+\Delta t)P(s, t+\Delta t) \ln\left[\frac{P(r, t+\Delta t)P(s, t+\Delta t)}{P^0(r)P^0(s)}\right] \tag{2.20}$$

and the unique additivity properties of the logarithmic function can now be exploited. Noting the normalization condition $\sum_m P(m, t) = 1$, equation (2.18) reduces immediately to

$$\sum_m P(m, t) \ln\left[\frac{P(m, t)}{P^0(m)}\right] \geqslant \sum_m P(m, t+\Delta t) \ln\left[\frac{P(m, t+\Delta t)}{P^0(m)}\right] \tag{2.21}$$

and hence we obtain the rate of entropy production

$$-\frac{d\Delta S}{dt} \geqslant 0. \tag{2.22}$$

Thus we see that the entropy deficiency has a definite rate of decay independent of the molecularity of the process; a result which stems from the unique additivity properties of the entropy. Furthermore, at equilibrium ΔS corresponds to the appropriate thermodynamic potential which, in the case of a closed system coupled to a heat bath, is the Helmholtz free energy. We add that if one merely wished to obtain the rate of entropy production (2.22) without considering convex functions in general, an alternative derivation is possible starting from the master equation corresponding to (2.8). This is shown in the Appendix.

3. VIBRATIONAL RELAXATION

We now investigate the relaxation of HF molecules in the presence of a buffer gas (heat bath) at 300 K. The rotational and translational (R–T) processes are assumed to be sufficiently rapid for these degrees of freedom to be considered in equilibrium with the heat bath. The remaining processes fall into two main categories. These are the V–V processes by which vibrational quanta are transferred between molecules, i.e.

$$\mathrm{HF}(n)+\mathrm{HF}(m)\rightarrow\mathrm{HF}(n+\Delta v)+\mathrm{HF}(m-\Delta v) \tag{3.1}$$

and V–T processes in which vibrational quanta are lost to (or gained from) the heat bath, i.e.

$$\mathrm{HF}(n)+\mathrm{HF}(m)\rightarrow\mathrm{HF}(n+\Delta v)+\mathrm{HF}(m-\Delta v') \tag{3.2}$$

where $\Delta v\neq\Delta v'$. We assume that although the buffer gas (e.g. Ar) is an efficient agent for R–T processes it is inefficient for vibrational relaxation and we therefore neglect V–T processes of the form $\mathrm{HF}(n)+\mathrm{Ar}\rightarrow\mathrm{HF}(m)+\mathrm{Ar}$. The vibrational energy levels of HF are anharmonic and taken to be Morse oscillator levels, i.e.

$$E_n=(n+\tfrac{1}{2})\hbar\omega-(n+\tfrac{1}{2})^2\,\hbar\omega x_e, \tag{3.3}$$

where for the frequency and anharmonicity we take the values $\omega=4138{\cdot}7\ \mathrm{cm}^{-1}$ and $x_e=0{\cdot}0218$ respectively [11]. Because of the anharmonicity the V–V processes are ' off resonance ' and a small amount of energy, the energy defect, is lost (or gained) to (or from) the heat bath. Thus, unlike V–V processes between harmonic oscillators, the mean vibrational energy is no longer a conserved quantity ; only the mean number of quanta is conserved [6, 7]. Furthermore, due to the anharmonicity, the V–V processes that excite quanta, e.g.

$$2\mathrm{HF}(n)\rightarrow\mathrm{HF}(n-1)+\mathrm{HF}(n+1),$$

are exothermic (this may be easily verified using equation (3.3)) and hence thermodynamically preferred. Thus for V–V processes the trend is towards population inversion in contrast to the V–T processes which favour de-excitation. It is the competition between these two opposing trends that leads to many of the characteristic features of the relaxation process.

3.1. *Master equation and rate constants*

We study the relaxation process by means of the non-linear master equation

$$\frac{dP(r,t)}{dt}=\sum_{s,m,n}\{k(r,s\leftarrow m,n)P(m,t)P(n.\,t)-k(m,n\leftarrow r,s)P(r,t)P(s,t)\}. \tag{3.4}$$

The rate constants $k(r,s\leftarrow m,n)$ for which $r+s=m+n$ correspond to V–V processes whereas we define V–T processes as all those for which $r+s\neq m+n$. We also mention that in this master equation the rate constants have been multiplied by the total molecular density N since the populations $P(r,t)$ are defined as $N(r,t)/N$ where $N(r,t)$ is the (time dependent) density of molecules in state r.

In order to solve equation (3.4) we need all the state-to-state rate constants. We use the exponential gap form [12]

$$k(r,s\leftarrow m,n)=Ak^0(r,s\leftarrow m,n)\exp\left(-\lambda|E_m+E_n-E_r-E_s|/kT\right) \tag{3.5}$$

where $k^0(r,s\leftarrow m,n)$ is the prior rate constant (computed on the basis that all quantum states are equally accessible) which increases with increasing energy defect $\Delta E = E_m + E_n - E_r - E_s$, A is a normalization factor and λ a measure of the deviation of k from k^0. The rate constants k have an obvious temperature dependence but it should also be remembered that A and k^0 are also temperature dependent.

A detailed description of this type of rate constant, and a means of evaluating (synthesizing) the parameters A and λ is given elsewhere [12]. For our study we normalize the rate constants such that $k(0, 0 \leftarrow 1, 0)$ has its experimental value of $1{\cdot}0 \times 10^{12}$ cm^3 mol^{-1} s^{-1} at 300 K and set λ equal to 0·5. Rate constants computed in this way with similar values of λ have been shown to compare quite well with the available experimental results for the first few levels of HF [13, 14]. In all calculations the total HF density was taken as $N = 5{\cdot}35 \times 10^{-8}$ mol cm^{-3} (1 torr, 300 K).

For low quantum numbers the V–V processes have much smaller energy defects and hence larger rate constants than the corresponding V–T processes. However, as the quantum numbers involved become larger the V–V energy defect increases and the V–T energy defect decreases. Eventually a crossing point, which will be temperature dependent, is reached after which it is the V–T rate constants that become dominant. In figure 1 we plot series of V–V and V–T rate constants which clearly illustrate this point.

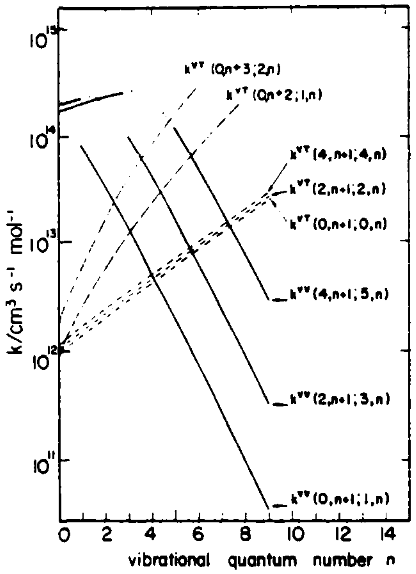

Figure 1. Series of V–V and V–T rate constants at 300 K. The rate constants are computed according to the exponential gap formula (3.5).

In order to keep our computations down to realistic proportions we include only the first 11 vibrational levels ($n = 0$ to 10). We retain all pairs of transitions $n + m \rightleftarrows r + s$ such that either the forward, $k(n, m \rightarrow r, s)$ or the reverse, $k(r, s \rightarrow n, m)$ rate constants are greater than or equal to $k(1, 0 \rightarrow 0, 0) = 10^{12}$ cm^3 mol^{-1} s^{-1} This still leaves us with over 300 (pairs of) rate constants including a number corresponding to multiple ($\Delta n = \pm 2, \pm 3, \pm 4$) quantum transitions, of the types (3.1) and (3.2). The role of the multiple V–V rate constants is discussed in § 3.2. Obviously, with a non-linear master equation, the number of rate constants increases enormously with the number of levels included.

The master equation was solved by direct numerical integration using a modified version of the 6th order Gear Hybrid, predictor-corrector, method.

3.2. *Population evolution*

We choose the initial distributions (which might have been formed, for example, by a pulse of radiation) to have a specified mean number of vibrational quanta, i.e.

$$\langle n \rangle_0 = \sum_n nP(n, 0). \tag{3.6}$$

In figures 2, 3, 4 we show the relaxation of three different distributions all with $\langle n \rangle_0 = 2$. We immediately see that in a very short time (about 0·3 μs) relative to the total relaxation time all initial distributions relax to virtually the same intermediate distribution (figures 2 (*d*), 3 (*d*), 4 (*d*)) which then develops more slowly and, quite obviously, independently of the initial distribution. The fact that the initial distributions in figures 3 and 4 are rather unphysical only serves

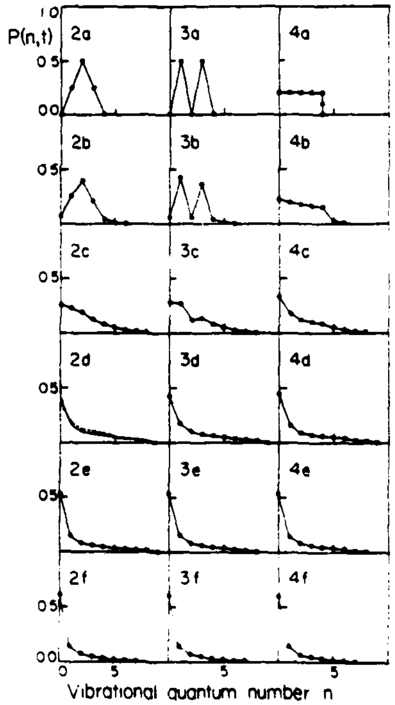

Figures 2, 3 and 4. Time evolution of the populations for different initial distributions having the same initial mean quantum numbers $\langle n \rangle_0 = 2$. Times are (for all figures): $a = 0{\cdot}00$, $b = 0{\cdot}02$, $c = 0{\cdot}10$, $d = 0{\cdot}31$, $e = 1{\cdot}01$, $f = 2{\cdot}02$ μs. The broken line in figure 2 (*d*) corresponds to a computation including only single quantum jump V–V rate constants.

to emphasize this point. The intermediate distribution, although not displaying strong population inversion shows a distinct smearing out of the distribution. The time scale for the first relaxation stage can be interpreted as follows: the lifetime of a vibrational level due to the V–V processes can be estimated as $\tau \sim 1/kN$ where k is the sum of all rate constants involving the given vibrational quantum numbers. On the average in our calculation each level participates in about 20 V–V processes while $k_{V-V} \sim 10^{13}$ cm^3 mol^{-1} s^{-1} and $N \simeq 5 \times 10^{-8}$ mol cm^{-3}, hence $\tau \sim 10^{-7}$ s.

In figure 2 (*d*) we have also marked the distribution that was obtained when including only single quantum jump ($\Delta n = \pm 1$) V–V rate constants in the master equation. To date, most computations have only included these rate constants [15, 16, 17] and we therefore investigated the effect of the multiple jump ones. Our general conclusion was that if only single jump rate constants are included, although all the basic features are still demonstrated, the degree of population inversion tended to be greater. We always included all multiple jump V–V rate constants of significant value in our calculations.

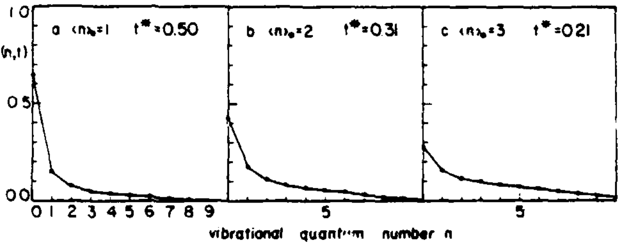

Figure 5. Intermediate quasi-equilibrium distributions observed for population evolution starting with different $\langle n \rangle_0$, t^* is the estimated time of attainment (in μs).

We also performed computations for initial distributions with mean quantum number $\langle n \rangle_0 = 3$ and $\langle n \rangle_0 = 1$. Again the same general phenomena observed for $\langle n \rangle_0 = 2$ were also apparent. We found, however, that the lower the initial number of quanta the longer it took to attain a first common intermediate distribution. In figure 5 we show the intermediate distributions obtained for $\langle n \rangle_0 = 1$, 2 and 3 with the approximate times of attainment. The reason why a distribution with a larger $\langle n \rangle_0$ should relax more quickly may simply be due to the fact that at higher quantum numbers more and more processes with larger rate constants (see figure 1) come into play.

Quite clearly, then, the relaxation process can be divided into two stages; a very fast V–V dominated stage giving rise to a quasi-equilibrium intermediate distribution and then a very much slower, V–T dominated relaxation process. The only important feature of the initial distribution seems to be the (mean) number of quanta, the precise form being apparently unimportant. The markedly different roles of the V–V and V–T processes and their different time scales can be illustrated quite strikingly by solving the master equation with either only V–V rate constants or only V–T rate constants included. This is shown in figure 6 which can be compared directly with figure 2 where all rate constants have been included. An additional feature of interest is that, in the case of V–V rate constants only, a population inversion or up-pumping process [6, 18] is

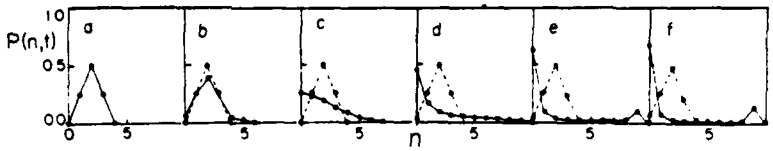

Figure 6. Time evolution of the populations with initial distribution as in figure 2 (*a*). Full line : V–V rate constants only. Broken line : V–T rate constants only.

starting to develop (figures 6 (*e*) and 6 (*f*)) that would in fact ultimately lead to dissociation (see § 4.2). However, it is precisely here that the V–T processes come into play and make this exceedingly inefficient.

In view of the very fast nature of the V–V stage there is the possibility of considerable differences in the observed initial vibrational distribution for a given experiment carried out under different conditions, e.g. measurement of the initial CO distribution in the highly exothermic chemical laser reaction $O+CS \rightarrow CO+S$ [19].

3.3. *Superposition*

In a number of relaxation processes where the energy defect is small compared with kT it has been found that the evolving population distribution can be represented as a linear superposition of initial and final distributions. For example, in cases of rotational relaxation [20] (which is a *linear* process) the rotational distribution was found to be well fitted by the form

$$P(J,t)=P^0(J)+[P(J,\ 0)-P^0(J)]\exp(-t/\tau), \tag{3.7}$$

where $P(J,0)$ is the initial (or nascent) distribution and $P^0(J)$ the final equilibrium distribution. A similar type of superposition was also found to give a good fit to the observed results of the vibrational relaxation of CO [7]. However, for this non-linear process the superposition was of the form

$$P(n,t)=P(n,t^*)+[P(n,0)-P(n,t^*)]\exp(-t/\tau), \tag{3.8}$$

where $P(n,t^*)$ is not the final equilibrium distribution but the distribution obtained when the V–V (but not the V–T) processes had reached equilibrium, i.e. a quasi-equilibrium intermediate distribution of the type discussed in the previous section.

Accordingly, we tried to fit our numerical results for the first, V–V dominated, stage of the relaxation of HF with a superposition of the form (3.8). We chose $P(n,0)$ to be of the form shown in figure 2 (*a*) ($\langle n\rangle_0=2$) and hence took $t^*=0{\cdot}31\ \mu s$ (see figure 2 (*d*)). In practice, the computation was performed by taking a fixed value of τ (which gives a measure of the relaxation time of the V–V process) and just fitted the final distribution $P(n,t^*)$. We found that the fitting was not very sensitive to the value of τ and for a wide range of values ($\tau^{-1}=10{\cdot}0$ to $20{\cdot}0\ \mu s^{-1}$) we obtained good results. In figure 7 we compare the exact, master equation results with the superposition (3.8) for $\tau^{-1}=14{\cdot}0\ \mu s^{-1}$. For the larger times the agreement is remarkably good.

Superpositions of the type described imply that the system retains a memory of the initial distribution during the relaxation process. Our results have shown

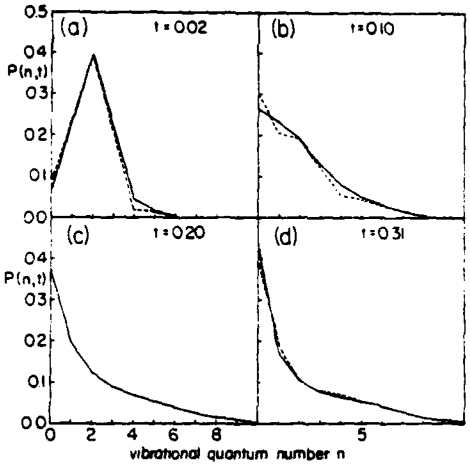

Figure 7. Comparison of exact population evolution (full line) with superposition model, equation (3.8) (broken line) for the first stage of the relaxation process (time in μs). Initial distribution as in figure 2 (*a*). In figure 7 (*c*) the two results are graphically indistinguishable (times in μs).

that beyond t^* the system apparently relaxes quite independently of $P(n, 0)$ and hence we cannot expect the superposition to hold beyond this time. This is not too surprising since now the relaxation is dominated by a different mechanism, namely the (large energy defect) V–T processes.

3.4. *Evolution of the moments*

So far we have only discussed the behaviour of microscopic quantities (the populations) and we now turn to the behaviour of macroscopic quantities, namely the moments. We consider the vibrational energy moments

$$\langle E_n{}^i(t)\rangle = \sum_n E_n{}^i\, P(n, t) \tag{3.9}$$

and the moments of vibrational quanta

$$\langle n^i(t)\rangle = \sum_n n^i P(n, t). \tag{3.10}$$

The first three of both are plotted (logarithmic ordinate for compaction) in figure 8. A number of interesting features are apparent. In the first stage of the process the second and third moments of both the energy and quantum number show a rapid increase. At much longer times they all decay in roughly the same manner. This is also true of the first moments but their early behaviour is very different. The energy actually shows almost pure exponential decay whereas the mean quantum number displays a different behaviour. If the first stage was a *pure* V–V process then $\langle n(t)\rangle$ should be constant; this actually appears to be approximately the case for the first few collisions.

In the last section we saw that the first stage of the relaxation could be fitted by a simple superposition (3.8). Hence all moments $(\langle M(t)\rangle)$ can easily be

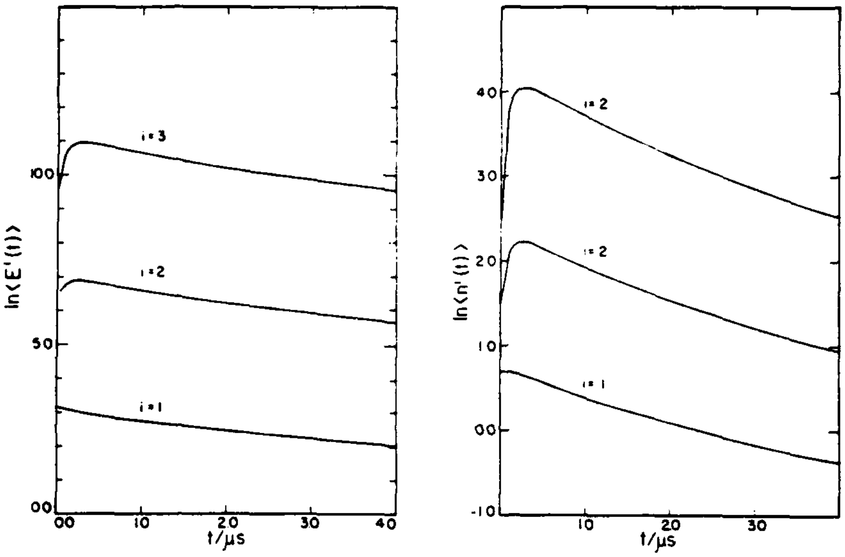

Figure 8. (*a*) Time evolution of the first three energy moments; $\langle E^i(t)\rangle$, $i=1, 2, 3$. At early times the first moment $\langle E(t)\rangle$ has almost pure exponential decay (time in μs). (*b*) Time evolution of the first three moments of vibrational quanta; $\langle n^i(t)\rangle$, $i=1, 2, 3$.

shown to relax in the following pure exponential manner

$$\langle M(t)\rangle=\langle M(t^*)\rangle+[\langle M(0)\rangle-\langle M(t^*)\rangle]\exp(-t/\tau), \qquad (3.11)$$

where $\langle M(0)\rangle$ and $\langle M(t^*)\rangle$ are the initial and quasi-equilibrium values of the moments respectively. If $M(t^*)$ is greater than $M(0)$, as was found to be the case for the second and third moments, then $\langle M(t)\rangle$ will increase from $t=0$ to $t=t^*$; otherwise it will decay. Although these general features are approximately displayed in figure 8 it is clear that the superposition cannot be the whole story. This is especially born out by the behaviour of the first moments. The almost pure exponential decay of $\langle E(t)\rangle$ would strongly support the superposition model but the different behaviour of $\langle n(t)\rangle$ could equally well contradict it!

The behaviour of the moments, or more generally the macroscopic observables, is of central importance in obtaining the maximal entropy distributions. This is described in the following section.

4. ENTROPY

We now turn to the use of entropy as a means of characterizing certain features of the relaxation process described in the previous sections.

4.1. *Entropy deficiency and vibrational entropy*

In figure 9 we plot the entropy deficiency (2.7) as a function of time for the relaxation processes corresponding to figure 2. As expected, ΔS shows a

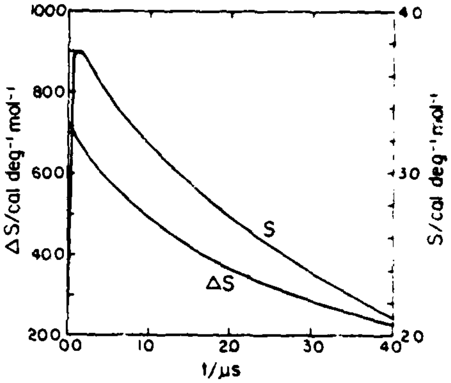

Figure 9. Time dependence of the entropy deficiency (left ordinate) and of the vibrational entropy (right ordinate) for population evolution with initial distribution as in figure 2 (*a*). The maximum in S corresponds to the smearing out of the population around figure 2 (*d*) (time in μs).

smooth monotonic decrease with the approach to equilibrium. Plots such as this are common to the relaxation of all the initial distributions examined.

In contrast to the entropy deficiency, the entropy of the vibrational distribution $S = -\sum_n P(n, t) \ln P(n, t)$ (as opposed to the entropy of the whole system, heat bath plus sub-system) does not necessarily have to display monotonic behaviour. In figure 9 we plot S as a function of time for the population evolution corresponding to figure 2. The sharp initial rise in S reflects the increase in entropy as the well ordered initial distribution (figure 2 (*a*)) relaxes to the smeared out intermediate distribution (figure 2 (*d*)). However, beyond this point the entropy then starts to decrease as the distribution narrows down towards the final equilibrium distribution. If one notes that the equilibrium distribution takes the form

$$P^0(n) = Q^{-1} \exp(-E_n/kT), \tag{4.1}$$

where Q is the partition function and T the (bath) temperature, then the entropy can be expressed in the following form :

$$\begin{aligned} S &= -\sum_n P(n, t) \ln P(n, t), \\ &= -\sum_n P(n, t) \ln \left[\frac{P(n, t)}{P^0(n)}\right] - \sum_n [P(n, t) - P^0(n)] \ln P^0(n) \\ &\qquad\qquad - \sum_n P^0(n) \ln P^0(n), \\ &= -\Delta S + \frac{1}{kT}[\langle E(t)\rangle - \langle E(\infty)\rangle] + S_0, \end{aligned} \tag{4.2}$$

where S_0 is the entropy of the equilibrium distribution, ΔS the entropy deficiency and the term $1/kT[\langle E(t)\rangle - \langle E(\infty)\rangle]$ represents the amount of entropy transferred to the heat bath. This equation enables us to represent ΔS in the form

$$\Delta S = \frac{1}{kT} \Delta E - (S - S_0). \tag{4.3}$$

The second law of thermodynamics requires that $\Delta S \geqslant 0$ and hence we must always have $\Delta E \geqslant kT(S-S_0)$. If we now consider just the first stage of the relaxation process and let S_0 represent the entropy of the quasi-equilibrium distribution we can deduce the following. In certain cases of strong population inversion we may have $S > S_0$ (as opposed to our case where $S < S_0$) and hence more entropy must be transferred to the heat bath to ensure $\Delta S \geqslant 0$. We can now see that this is facilitated by having a lower temperature T. Hence we can draw the general conclusion that the lower the bath temperature the greater the possible population inversion.

4.2. *The maximal entropy distribution*

Finally we examine the maximal entropy procedure as a means of reproducing the evolving population distribution. It has been shown that this procedure is of a variational type and that the maximal entropy distribution will converge monotonically to the exact one as more and more (independent) constraints are included [2, 3]. Clearly the procedure will be most useful when one can obtain accurate results using the least number of constraints. Hence our aim is to find those constraints that contain the most information pertinent to the relaxation process.

The results of § 3.4 show that the behaviour of the moments $\langle E_n(t)\rangle$ and $\langle n(t)\rangle$ reflect quite a few features of the relaxation process and particularly the early V–V stage. Accordingly, as a first attempt to find a suitable maximal entropy distribution we maximize the entropy $S = -\sum_n P(n,t)\ln P(n,t)$ subject to the constraints $\langle E_n(t)\rangle$ and $\langle n(t)\rangle$. This standard procedure yields

$$P(n,t) = Q^{-1}\exp\left[-\lambda_1(t)E_n - \lambda_2(t)n\right], \tag{4.4}$$

where λ_1 and λ_2 are time dependent Lagrange multipliers and Q the (time dependent) partition function. The precise behaviour of $\lambda_1(t)$ and $\lambda_2(t)$ will depend on the behaviour of the corresponding moments but we do know the asymptotic behaviour, i.e.

$$\lambda_1(t) = 1/kT \quad \text{and} \quad \lambda_2(t) = 0 \quad (t \to \infty), \tag{4.5}$$

where T is the bath temperature. The distribution (4.4) resembles that suggested by Treanor *et al.* [6] to describe the quasi-stationary state that would be obtained for a pure V–V relaxation process. However, in our case we are interested in obtaining the form of the distribution function that is valid throughout the entire relaxation process and not just the quasi-stationary distribution.

Returning to the distribution (4.4) we can rewrite it in the form

$$P(n,t) = Q^{-1}\exp\left[-\lambda_1(t)(E_n - E_n{}^0) - \lambda_3(t)E_n{}^0\right], \tag{4.6}$$

where $E_n{}^0$ is the harmonic oscillator energy level,

$$E_n{}^0 = (n+\tfrac{1}{2})\hbar\omega, \quad \text{and} \quad \lambda_3(t) = [\lambda_1(t) + \lambda_2(t)/\hbar\omega].$$

Since $E_n < E_n{}^0$ we see that for sufficiently large λ_1 (depending, of course, on the behaviour of λ_3) $P(n,t)$ can display strong (in fact diverging) population inversion. Note that in the limit of zero anharmonicity (4.4) reduces to the canonically invariant form [1]

$$P(n, t) = Q^{-1} \exp\left[-\lambda_1(t) E_n{}^0\right];$$

the multiplier $\lambda_2(t)$ has vanished since $\langle n \rangle$ is no longer an informative moment, now being (trivially) linearly dependent on $\langle E_n{}^0 \rangle$. Although the two-parameter distribution (4.4) may be adequate at short times it will break down at large ones since it fails to take into account the de-excitation of higher vibrational levels by the V–T processes. Clearly additional constraints are required. One might consider trying $\langle n^2(t) \rangle$ but this is not informative since it is linearly dependent on $\langle E_n \rangle$ and $\langle n \rangle$ (see equation (3.3)). We can, however, use $\langle E_n{}^2(t) \rangle$ and in figures 10 and 11 we compare the exact distribution at a number of times with the maximal entropy distributions using $\langle E_n(t) \rangle$ and $\langle n \rangle$, and $\langle E_n(t) \rangle$, $\langle n(t) \rangle$ and $\langle E_n{}^2(t) \rangle$ as constraints. It can be seen that the three-parameter distribution gives a good fit to the exact one for all times shown. As expected, the two-parameter distribution, although adequate at very short times, is particularly poor at longer times. Clearly though, other combinations of constraints are possible. We also compared (not shown) the exact distributions with those using $\langle E_n(t) \rangle$ and $\langle E_n{}^2(t) \rangle$ and $\langle E_n(t) \rangle$, $\langle E_n{}^2(t) \rangle$ and $\langle E_n{}^3(t) \rangle$ as constraints. The latter distribution gives excellent results and one must conclude that this combination of constraints contains more information than the other three-parameter distribution tried. This is perhaps not surprising since the combination $\langle E_n \rangle$, $\langle E_n{}^2 \rangle$ and $\langle E_n{}^3 \rangle$ implicitly contains information about all vibrational moments up to $\langle n^6 \rangle$ whereas $\langle E_n \rangle$, $\langle n \rangle$ and $\langle E_n{}^2 \rangle$ only includes terms up to $\langle n^4 \rangle$. However, our results should be considered as phenomenological at this stage and we have simply shown that the evolving population distribution can be accurately fitted with a three-parameter distribution. Our choice of constraints has been guided by physical intuition but we cannot tell at this stage whether there are other combinations of constraints that would be more informative and hence give even better results. Finally, we mention that

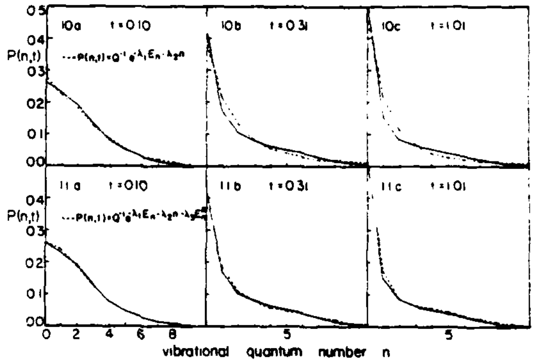

Figures 10 and 11. Comparison of exact (full line) distributions with two (figure 10) and three (figure 11) constraints maximal entropy distributions (broken line) at a number of times (μs). The third constraint is almost linearly dependent on the previous ones (cf. [21] for the definition of linear dependence and its implications).

the numerical determination of the Lagrange multipliers was carried out by means of a recently devised linear programming technique [21].

4.3. *Constraints*

The previous discussion clearly identified the procedure that is still missing in the maximal entropy formalism. One needs to be able to identify the constraints directly without computing the probabilities first. For the time evolution under the Liouville equation this procedure has already been implemented [22]. It is thus possible to obtain an exact solution of the Liouville equation via the maximal entropy formalism. Work is in progress on deriving corresponding results for the master equation. Until such results are available, the role of the maximal entropy formalism is either that of providing a compact expressions for the populations or that of inducing the most likely (or most conservative or least biased) population distribution subject to given average values of a few constraints (which, by themselves, do not suffice to determine uniquely the distribution). The procedure that is still missing specifies a set of constraints whose average values, when used in the maximal entropy formalism, determine an exact solution of the master equation.

5. Concluding remarks

We have investigated the vibrational relaxation of diatomic molecules in a heat bath by direct numerical integration of the master equation, using a comprehensive set of exponential gap state-to-state rate constants. The anharmonicity of the energy levels gives rise to a number of interesting features ; principally, that the relaxation process can be divided into two stages : first, a very fast up-pumping stage dominated by V–V exchange collisions which leads to a type of quasi-equilibrium intermediate distribution and secondly, a very much slower V–T dominated stage during which the intermediate distribution relaxes towards thermal equilibrium. This second stage appears to be quite independent of the precise form of the initial distribution. The first stage can be fitted quite well by a linear superposition of the initial and quasi-equilibrium distributions. The evolution of the moments of energy and vibrational quanta reflect the various stages of the relaxation process. We then proceeded to show how entropy can be used to characterize the relaxation process. The entropy deficiency displays a smooth monotonic decay with the approach to equilibrium. On the other hand, the entropy of the relaxing subsystem need not display monotonic decay and, indeed, varies according to the relative ordering of the evolving population distribution. The maximal entropy distribution was used to describe the evolving population distribution. Although a two-constraint distribution provided an adequate fit to the V–V dominated stages of the relaxation it was found necessary to add at least a third constraint to account for later, V–T dominated, stages of the process.

Although further numerical work would be of interest ; e.g. to consider the effect of changes of temperature and other parameters, more theoretical work is called for. At the kinetic level it is of great practical importance to devise models that will explain the transition from V–V dominated to V–T dominated collisions and hence predict the degree of possible population inversion. At the thermodynamic level it is important to devise criteria for selecting the most informative constraints in order to obtain the most accurate maximal entropy distributions.

We may also point out that the procedures outlined here for computing vibrational state populations evolving in time subject to V–V and V–T relaxation may be of great utility in numerical modelling of chemical lasers [23]. In these models, a great deal of computational effort is expended in calculating state-to-state rate constants and in solving non-linear master equations of the type of equation (3.4). We suggest that incorporation of explicit expressions for $dP(n)/dt$ would greatly reduce the time required for these modelling calculations.

We would like to thank Ms. S. Feliks and Ms. V. Buch for computational assistance and Mr. N. Agmon and Mr. Y. Alhassid for the use of their maximal entropy programme. M.T. thanks the Royal Society for a Research Fellowship. This work reflects research supported by U.S. Air Force Grants AFOSR 77–3135 (R.D.L.) AFOSR-EOARD 77–062 (A.B-S.) and AFOSR 75–2758 (J.I.S.).

APPENDIX

It is a simple matter to show [1] the equivalence between the stochastic equation

$$P(r, t+\Delta t) = \sum_{s,\,m,\,n} \Pi(rs|mn)P(m, t)P(n, t) \tag{A 1}$$

and the non-linear master equation

$$\frac{dP(r, t)}{dt} = \sum_{s,\,m,\,n} \{k(r, s\leftarrow m, n)P(m, t)P(n, t) - k(m, n\leftarrow r, s)P(r, t)P(s, t)\}. \tag{A 2}$$

The state-to-state rate constants $k(r, s\leftarrow m, n)$ satisfy the condition of detailed balance with the equilibrium distributions, i.e.

$$k(r, s\leftarrow m, n)P^0(m)P^0(n) = k(m, n\leftarrow r, s)P^0(r)P^0(s). \tag{A 3}$$

Using this condition the master equation (A 2) can be rewritten in the following form

$$\frac{dP(r, t)}{dt} = \sum_{s,\,m,\,n} k(r, s\leftarrow m, n)P^0(m)P^0(n)\left[\frac{P(m, t)P(n, t)}{P^0(m)P^0(n)} - \frac{P(r, t)P(s, t)}{P^0(r)P^0(s)}\right]. \tag{A 4}$$

We wish to find the rate of entropy production $-d\Delta S/dt$, i.e.

$$-\frac{d\Delta S}{dt} = -\frac{d}{dt}\sum_r P(r, t)\ln\left[\frac{P(r, t)}{P^0(r)}\right] = -\sum_r \frac{dP(r, t)}{dt}\ln\left[\frac{P(r, t)}{P^0(r)}\right], \tag{A 5}$$

which we write in the ' symmetrized ' form

$$\begin{aligned}-\frac{d\Delta S}{dt} = &-\tfrac{1}{4}\sum_r \frac{dP(r, t)}{dr}\ln\left[\frac{P(r, t)}{P^0(r)}\right] - \tfrac{1}{4}\sum_s \frac{dP(s, t)}{dt}\ln\left[\frac{P(s, t)}{P^0(s)}\right]\\ &-\tfrac{1}{4}\sum_m \frac{dP(m, t)}{dt}\ln\left[\frac{P(m, t)}{P^0(m)}\right] - \tfrac{1}{4}\sum_n \frac{dP(n, t)}{dt}\ln\left[\frac{P(n, t)}{P^0(n)}\right].\end{aligned} \tag{A 6}$$

By using the master (A 4) we can reduce (A 6) to

$$-\frac{d\Delta S}{dt}=\frac{1}{4}\sum_{r,\,s,\,m,\,n} k(r,\,s\leftarrow m,\,n)P^0(m)P^0(n)\left[\frac{P(m,\,t)P(n,\,t)}{P^0(m)P^0(n)}-\frac{P(r,\,t)P(s,\,t)}{P^0(r)P^0(s)}\right]$$

$$\times\left\{\ln\left[\frac{P(m,\,t)P(n,\,t)}{P^0(m)P^0(n)}\right]-\ln\left[\frac{P(r,\,t)P(s,\,t)}{P^0(r)P^0(s)}\right]\right\} \qquad \text{(A 7)}$$

and since $(x-y)(\ln x-\ln y)\geqslant 0$ we have the desired result

$$-\frac{d\Delta S}{dt}\geqslant 0. \qquad \text{(A 8)}$$

An interesting difference between this derivation and the more general one described in § 2 is that here it is necessary to invoke the detailed balance condition (A 3).

REFERENCES

[1] OPPENHEIM, I., SHULER, K. E., and WEISS, G. H., 1967, *Adv. molec. Relax. Process.*, **1**, 13.
[2] LEVINE, R. D., 1976, *J. chem. Phys.*, **65**, 3302.
[3] PROCACCIA, I., SHIMONI, Y., and LEVINE, R. D., 1976, *J. chem. Phys.*, **65**, 3284.
[4] BERNSTEIN, R. B., and LEVINE, R. D., 1975, *Adv. atom. molec. Phys.*, **11**, 215.
[5] BEN-SHAUL, A., LEVINE, R. D., and BERNSTEIN, R. B., 1972, *J. chem. Phys.*, **57**, 5427.
[6] TREANOR, C. E., RICH, J. W., and REHM, R. G., 1968, *J. chem. Phys.*, **48**, 1798.
[7] LEVINE, R. D., and BEN-SHAUL, A., 1977, *Chemical and Biochemical Applications of Lasers*, Vol. 2, edited by C. B. Moore (Academic Press), p. 145.
[8] RUBINSON, M., and STEINFELD, J. I., 1974, *Chem. Phys.*, **4**, 467.
[9] PROCACCIA, I., and LEVINE, R. D., 1975, *J. chem. Phys.*, **62**, 2496.
[10] MORIMOTO, T., 1963, *J. phys. Soc. Japan*, **18**, 328.
[11] HERZBERG, G., 1950, *Spectra of Diatomic Molecules*, Vol. 1, 2nd edition (Van Nostrand).
[12] PROCACCIA, I., and LEVINE, R. D., 1975, *J. chem. Phys.*, **63**, 4261.
[13] CLENDENING, C., STEINFELD, J. I., and WILSON, L. E., 1976, AFWL-TR-76-144.
[14] SCHMAILZL, U., 1977, Ph.D. Thesis, Max-Planck Gesellschaft Project Gruppe für Laser Forschung.
[15] BRAY, K. N. C., 1968, *J. Phys.* B, **1**, 705.
[16] BRAY, K. N. C., 1970, *J. Phys.* B, **3**, 1515.
[17] CALEDONIA, G. E., and CENTER, R. E., 1971, *J. chem. Phys.*, **55**, 552.
[18] PUMMER, H., PROCH, D., SCHMAILZL, U., and KOMPA, K. L., 1976, *Optics Commun.*, **19**, 273.
[19] KELLEY, J. D., 1976, *Chem. Phys. Lett.*, **41**, 7.
[20] PROCACCIA, I., SHIMONI, Y., and LEVINE, R. D., 1975, *J. chem. Phys.*, **63**, 3181.
[21] ALHASSID, Y., AGMON, N., and LEVINE, R. D., 1978, *Chem. Phys. Lett.*, **53**, 22.
[22] ALHASSID, Y., and LEVINE, R. D., 1977, *J. chem. Phys.*, **67**, 4321.
[23] EMANUEL, G., 1976, *Handbook of Chemical Lasers*, edited by R. W. F. Gross and J. F. Bott (Wiley-Interscience), p. 469-549.

Volume 61, number 3 CHEMICAL PHYSICS LETTERS 1 March 1979

ON EQUILIBRIUM DISTRIBUTIONS AND DETAILED BALANCE RELATIONS IN NON-ISOTHERMAL SYSTEMS *

A. BEN-SHAUL and M. TABOR **
Department of Physical Chemistry, The Hebrew University, Jerusalem, Israel

Received 19 April 1978
Revised manuscript received 10 November 1978

The significance of the detailed balance principle and equilibrium solutions of the master equation is discussed from a thermodynamic point of view for isolated and isothermal systems. Starting from a master equation for all the time dependent degrees of freedom it is shown that the uniqueness of the equilibrium distribution as a stationary solution is ensured if the detailed rate constants are balanced with the aid of the distribution which maximizes the entropy subject to the thermodynamic constraints. This procedure should precede physical assumptions which simplify the original master equation, e.g. the assumption that rapidly relaxing modes can be described by canonical distribution functions.

1. Introduction

In most types of molecular relaxation phenomena it is possible to distinguish between rapidly and slowly relaxing degrees of freedom. For example, translational and rotational relaxation of molecules in the gas phase can usually be regarded as instantaneous on the time scale of vibrational relaxation. Whenever such separation to different time scales is justified the approach to equilibrium of the slowly relaxing modes is governed by a master equation with temperature dependent rate constants. The temperature characterizes the distribution over the rapidly relaxing modes. If the system is coupled to a heat bath this temperature is constant. In the more general case it is time dependent and reflects the instantaneous average energy content of these modes. A definite, temperature dependent, relationship of the same formal appearance, known commonly as the detailed balance principle, connects the forward and reverse rate constants for both isothermal and nonisothermal systems.

The detailed balance principle is a consequence of the requirement that at thermodynamic equilibrium the rates of forward and reverse detailed processes are equal [1]. Since the equilibrium condition is uniquely determined by the macroscopic thermodynamic constraints so also is the detailed balance relationship. Based on this fact we shall argue below that the interpretation of the relation between the rate constants mentioned above as detailed balancing is valid for isothermal systems but can be (and has been) misleading for nonisothermal systems. This distinction is not just semantic. Related, but more serious, misconceptions may arise with respect to the stationary, equilibrium, solutions of the master equation; in particular when besides the ordinary canonical constraints the equilibrium distribution is determined by additional constraints.

In the following we show that a proper (macroscopic) description of a molecular relaxation process should start with the following procedure: (a) A master equation is written for all the time dependent degrees of freedom. (b) The equilibrium distribution is determined by maximizing the system entropy subject to the appropriate thermodynamic constraints. (c) The equilibrium distribution is used to determine the detailed balance relation, thereby

---

* Work supported by the European Office of Aerospace Research and Development (AFSC) of the USAF, Grant No. EOARD 77-062.

** Present address: Department of Chemistry, University of Illinois, Urbana, Illinois 61801, USA.

ensuring the uniqueness of the equilibrium distribution as a stationary solution. Additional assumptions (like instantaneous relaxation of certain modes), can be made after the three basic requirements have been fulfilled.

As an example to serve us throughout the discussion we take a gas of N diatomic molecules in volume V. For the sake of concreteness it can be assumed that the initial nonequilibrium condition of the system is the result of vibrational excitation (e.g. following infrared laser irradiation). Neglecting radiative, wall and other secondary effects the molecules will relax to a new equilibrium state via bimolecular collisions. If the system is thermally isolated (or "adiabatic") the new final temperature will differ from the original temperature before the excitation. The temperatures are equal if the system is coupled to a heat bath ("isothermal"). We shall treat in detail the adiabatic system and briefly the isothermal one. (The nature of the heat bath will not be specified; usually it is realized by a buffer gas in excess.) The Treanor distribution [2] which characterizes an intermediate ("quasi-equilibrium"), stage in the relaxation of anharmonic oscillators will also be discussed.

2. Equilibrium and detailed balance

The general form of the master equation describing a relaxation process caused by binary collisions between molecules of the same kind is

$$\mathrm{d}P(a)/\mathrm{d}t = -\rho \sum_{b,a',b'} [k(a,b \to a',b')P(a)\,P(b) - k(a',b' \to a,b)\,P(a')\,P(b')]\,, \tag{1}$$

where a represents all the degrees of freedom that may change during the relaxation. The summation symbol stands also for integration when a involves continuous variables. $\rho = N/V$ is the gas density, $P(a)$ is the probability of finding a molecule in state a and the k's are the rate constants.

The equilibrium solution of (1), $P_0(a)$, is the (unique) distribution function $P(\alpha)$ which maximizes the entropy [3]

$$S = -Nk \sum_a P(a) \ln[P(a)/g(a)]\,, \tag{2}$$

subject to the thermodynamic constraints on the system. k is the Boltzmann constant. $g(a)$, the degeneracy of a, involves density of state factors for continuous degrees of freedom. To ensure that $P_0(a)$ is the equilibrium solution, $\mathrm{d}P_0(a)/\mathrm{d}t = 0$, the rate constants must satisfy the detailed balance relation

$$P_0(a)\,P_0(b)\,k(a,b \to a',b') = P_0(a')\,P_0(b')\,k(a',b' \to a,b). \tag{3}$$

We turn now to the special case of diatomic molecules. To simplify the discussion the state of a molecule will be specified by $a = \epsilon, n$, $(b = e, m)$, where $\epsilon = \epsilon_t + \epsilon_r$ is the sum of translational and rotational energies and n is the vibrational level. The master equation is

$$\begin{aligned}\mathrm{d}P(\epsilon,n)/\mathrm{d}t = -\rho \sum_{m,n',m'} \int \mathrm{d}e\,\mathrm{d}\epsilon'\,\mathrm{d}e'\,[&k(\epsilon,n,e,m \to \epsilon',n',e',m')P(\epsilon,n)P(e,m) \\ &- k(\epsilon',n',e',m' \to \epsilon,n,e,m)\,P(\epsilon',n')P(e',m')]\,,\end{aligned} \tag{4}$$

where $P(\epsilon, n)\,\mathrm{d}\epsilon$ is the probability of finding a molecule in vibrational state n and translational–rotational (t/r) energy between ϵ and $\epsilon + \mathrm{d}\epsilon$,

$$\sum_n \int P(\epsilon,n)\,\mathrm{d}\epsilon = \sum_n P(n) = \int P(\epsilon)\,\mathrm{d}\epsilon = 1. \tag{5}$$

It should be noticed that since in each bimolecular collision the total collision energy is conserved the detailed rate constants are nonzero only when $\epsilon + e + \epsilon_n + \epsilon_m = \epsilon' + e' + \epsilon_{n'} + \epsilon_{m'}$. (The rate constants contain a "built in" $\delta(\epsilon + e + \epsilon_n + \epsilon_m - \epsilon' - e' - \epsilon_{n'} - \epsilon_{m'})$ factor [1].)

The entropy (per molecule) is given by

$$S = -k\sum_n \int d\epsilon P(\epsilon, n)[P(\epsilon, n)\ln[P(\epsilon, n)/\rho(\epsilon)], \tag{6}$$

where $\rho(\epsilon)$ is the density of t/r states [3].

In an isolated system the average energy per molecule is kept constant throughout the relaxation process. That is

$$\langle \epsilon + \epsilon_n \rangle = \sum_n \int d\epsilon P(\epsilon, n)(\epsilon + \epsilon_n) = A, \tag{7}$$

where the constant A is the initial (as well as final) value of the average energy per molecule E/N. (In the example of nonequilibrium created by laser excitation, E is the energy of the gas after the excitation.)

The equilibrium distribution $P_0(\epsilon, n)$ is the one which maximizes the entropy, (6), subject to the normalization and energy constraints, (5) and (7) respectively. The maximization procedure is standard and yields

$$P_0(\epsilon, n) = \rho(\epsilon)\exp[-\beta_0(\epsilon + \epsilon_n)]/Q(\beta_0) = P_0(\epsilon)P_0(n), \tag{8}$$

$$P_0(\epsilon) = \rho(\epsilon)\exp(-\beta_0\epsilon)/q_t(\beta_0), \quad P_0(n) = \exp(-\beta_0\epsilon_n)/q_v(\beta_0), \tag{9}$$

where $Q(\beta_0) = q_t(\beta_0)q_v(\beta_0)$ is the partition function per molecule corresponding to the final equilibrium temperature $T_0 = (k\beta_0)^{-1}$. T_0, the common temperature of all the degrees of freedom at $t \to \infty$ is uniquely determined through

$$\langle \epsilon + \epsilon_n \rangle_{\text{eq}} = -\partial \ln Q(\beta_0)/\partial\beta_0 = A, \tag{10}$$

where $-\partial \ln Q(\beta_0)/\partial\beta_0 \equiv -\partial \ln Q(x)/\partial x$ at $x = \beta_0$.

Using (3) (with $a = \epsilon, n$) and (8) and recalling that the rate constants vanish unless $\epsilon + \epsilon_n + e + \epsilon_m = \epsilon' + \epsilon_{n'} + e' + \epsilon_{m'}$, we find

$$\rho(\epsilon)\rho(e)k(\epsilon, \epsilon_n, e, \epsilon_m \to \epsilon', \epsilon_{n'}, e', \epsilon_{m'}) = \rho(\epsilon')\rho(e')k(\epsilon', \epsilon_{n'}, e', \epsilon_{m'} \to \epsilon, \epsilon_n, e, \epsilon_m). \tag{11}$$

This is the basic detailed balance relation for the bimolecular relaxation process. Exactly the same expression can be derived from microscopic considerations based on the symmetry properties of the state-to-state transition probabilities. In this case (11) is known as the principle of microscopic reversibility.

3. The reduced master equation

The full master equation, (4), and detailed balance relation, (11), can be simplified by assuming that t/r relaxation is instantaneous compared to vibrational relaxation. That is, $P(n) = \int P(\epsilon, n)\, d\epsilon$ relaxes more slowly than $P(\epsilon) = \sum P(\epsilon, n)$. This means that at every stage of the relaxation

$$P(\epsilon, n) = P(n)P_c(\epsilon) = P(n)\rho(\epsilon)\exp(-\beta\epsilon)/q_t(\beta). \tag{12}$$

It should be noted that the instantaneous t/r temperature $T = (k\beta)^{-1}$ which characterizes the canonical distribution $P_c(\epsilon)$ is time dependent, i.e. $\dot{\beta} \neq 0$ except at $t \to \infty$ when $\beta = \beta_0$, see below. Substitution of (12) into (4) and integration yield

$$dP(n)/dt = -\rho \sum_{m,n',m'} [k(n, m \to n', m'; \beta)P(n)P(m) - k(n', m' \to n, m; \beta)P(n')P(m')] . \tag{13}$$

The, time dependent, averaged rate constants in this equation are given by

$$k(n, m \to n', m'; \beta) = \int \mathrm{d}\epsilon \, \mathrm{d}e \, \mathrm{d}\epsilon' \, \mathrm{d}e' \, P_{\mathrm{c}}(\epsilon) \, P_{\mathrm{c}}(e) \, k(\epsilon, n, e, m \to \epsilon', n', e', m'). \tag{14}$$

The time dependence of this rate constant is due to the time dependence of β in $P_{\mathrm{c}}(\epsilon)$, (12). Multiplying each $\rho(\epsilon)$ factor in (11) by $\exp(-\beta\epsilon)/q_{\mathrm{t}}(\beta)$ to get $P_{\mathrm{c}}(\epsilon)$, integrating over $\epsilon, e, \epsilon', e'$ and recalling that $k(\epsilon, n, e, m \to \epsilon', n', e', m')$ is zero for $\epsilon + \epsilon_n + e + \epsilon_m + \epsilon' + \epsilon_{n'} + e' + \epsilon_{m'}$ we find

$$\exp[-\beta(\epsilon_n + \epsilon_m)] \, k(n, m \to n', m'; \beta) = \exp[-\beta(\epsilon_{n'} + \epsilon_{m'})] \, k(n', m' \to n, m; \beta). \tag{15}$$

A relation of exactly this form accounts for the detailed balance principle in isothermal systems where $\beta = \mathrm{const} = 1/kT_{\mathrm{b}}$ and T_{b} is the heat bath temperature. However, while in the isothermal case (15) is a direct result of the fundamental relation (3) (see below), its derivation for isolated systems was based on the extra assumption (12). We emphasize this difference because a general detailed balance relation is unique, time independent and should directly reflect the equilibrium distribution. Thus, while in the isothermal case comparison of (3) and (15) correctly implies that the equilibrium distribution is

$$P_{\mathrm{c}}(n) = \exp(-\beta\epsilon_n)/q_{\mathrm{v}}(\beta), \tag{16}$$

the identification of (16) as the equilibrium distribution in the isolated system is erroneous. Furthermore, this misleading conclusion may appear to be supported by the fact that direct substitution of (16) into the reduced master equation (13) (as suggested for example in ref. [2]), yields for any β, $\mathrm{d}P_{\mathrm{c}}(n)/\mathrm{d}t = 0$, as if (16) was an equilibrium solution. This contradicts the assertion that (8), in which $\beta_0 \neq \beta(t \neq \infty)$, is the only equilibrium solution. On the other hand, taking the time derivative of (16) we find

$$\dot{P}_{\mathrm{c}}(n) = -(\epsilon_n - \langle\epsilon_n\rangle)\dot{\beta} P_{\mathrm{c}}(n), \tag{17}$$

where $\langle\epsilon_n\rangle = -\partial \ln q_{\mathrm{v}}/\partial\beta$. Hence $P_{\mathrm{c}}(n)$ is a stationary solution only when $\dot{\beta} = 0$ (i.e. at $t \to \infty$ when $\beta = \beta_0$).

The resolution of this "paradox" is indeed quite simple. We shall now show that (16) should be excluded not only as a stationary solution but also as a transient distribution. This is because the reduced master equation, (13), does not fully characterize the relaxation process and must be solved simultaneously with the equation for $\dot{\beta} = -\dot{T}/kT^2$. The rate equation for β is obtained from the energy conservation constraint, (7), and the master equation, (13). Using $\dot{A} = \langle\dot{\epsilon}\rangle + \langle\dot{\epsilon}_n\rangle = 0$ and (12) we find

$$\dot{T} = -(1/C_v^{\mathrm{tr}})\langle\dot{\epsilon}_n\rangle, \tag{18}$$

where $\langle\dot{\epsilon}_n\rangle$ can be evaluated from (13) after multiplying by ϵ_n and summing over n. C_v^{tr} is the t/r heat capacity per molecule, $C_v^{\mathrm{tr}} \approx (5/2k)$. If at some moment the vibrational distribution was of the form (16) we would get $\langle\dot{\epsilon}_n\rangle = C_v^{\mathrm{vib}}\dot{T}$. From (18) it is obvious that this value and hence (16) are absurd (except of course at $t \to \infty$ when $\dot{T} = 0$, $T = 1/k\beta_0$). Thus, although by direct substitution into the reduced master equation the canonical-like distribution (16) may appear as an equilibrium solution this possibility is overruled since it violates (7) and (18). (Obviously $\mathrm{d}P(n)/\mathrm{d}t = 0$ alone does not imply that $P(n)$ is stationary. If this was sufficient then $P(n) \equiv 0$ is also stationary.)

An alternative proof of the above assertions, emphasizing that the t/r distribution and the vibrational distribution cannot be simultaneously canonical with the same temperature, except at $t \to \infty$, follows from (10). To simplify the arguments we can use, with no loss of generality, the classical expressions $Q = q_{\mathrm{t}}q_{\mathrm{v}}$. Using (8), (9) and (10) we find $A = \langle\epsilon\rangle_{\mathrm{eq}} + \langle\epsilon_n\rangle_{\mathrm{eq}} = 7/2\beta_0 = \frac{7}{2}kT_0$. If as assumed in (16) the t/r modes are Boltzmann throughout the relaxation then $\langle\epsilon_n\rangle = A - 5/2\beta = \frac{7}{2}kT_0 - \frac{5}{2}kT$. Suppose now that $P(n)$ is also canonical with vibrational temperature $T_{\mathrm{v}} = 1/k\beta_{\mathrm{v}}$ so that $\langle\epsilon_n\rangle = kT_{\mathrm{v}} = \frac{7}{2}kT_0 - \frac{5}{2}kT$. Thus, as long as the relaxation process has not been terminated $T_{\mathrm{v}} \neq T \neq T_0$ whereas at equilibrium $T_{\mathrm{v}} = T = T_0$.

4. Isothermal relaxation

If the system is coupled to a heat bath at temperature $T_b = (k\beta_b)^{-1}$ and t/r relaxation is instantaneous $P(\epsilon)$ is given by the canonical form (16) with $\beta = \beta_b$ = constant. Thus, only $P(n)$ is time dependent and the basic master equation is (1) with $a = n$. In this case $\langle\epsilon\rangle = -\partial \ln q_t(\beta_b)/\partial\beta_b$ = const but $\langle\epsilon_n\rangle$ is time dependent, hence $\langle\epsilon + \epsilon_n\rangle$ is not conserved during the relaxation. The conserved quantity is the total energy of the system + heat bath. It can be shown (see e.g. ref. [4]) that in this case the thermodynamic constraint defining the equilibrium state is $\langle\epsilon_n\rangle_{eq} = -\partial \ln q_v(\beta_b)/\partial\beta_b$. Maximization of (2), with $a = n$, subject to this constraint and the normalization condition $\Sigma P(n) = 1$, yields, as expected, the canonical distribution $P_0(n) = \exp(-\beta_b\epsilon_n)/q_v(\beta_b)$, cf. (16). Finally, using this result in (3) we find a detailed balance relation identical to (15) but with $\beta = \beta_b$ = constant. Of course, in the isothermal case (18) is identically zero and the reduced equation (13), with $\beta = \beta_b$, fully describes the relaxation process.

5. The Treanor distribution

The well known Treanor distribution [2] can be regarded as the equilibrium distribution of a hypothetical system in which only v–v collisions cause the relaxation. (This "quasistationary" distribution provides an approximate description of the vibrational populations at the end of the fast relaxation stage governed by v–v collisions. It is appropriate only for low lying levels for which $\tau_{vv} \ll \tau_{vt}$.) In an isolated system relaxing in this fashion the normalization, (5), and the energy conservation, (7), constraints should be supplemented by the quanta conservation constraint [2,3]

$$\langle n\rangle = \sum_n \int d\epsilon P(\epsilon, n) n = \sum_n nP(n) = B\,, \tag{19}$$

where B is the average number of vibrational quanta per molecule at $t = 0$, i.e. after the excitation. The equilibrium, Treanor, distribution obtains by maximizing (6) subject to (5), (7) and (19). This yields

$$P_0(\epsilon, n) = \rho(\epsilon)\exp[-\beta'(\epsilon + \epsilon_n) - \gamma' n]/Q(\beta', \gamma') = P_0(\epsilon)P_0(n), \tag{20}$$

$$P_0(\epsilon) = \rho(\epsilon)\exp(-\beta'\epsilon)/q_t(\beta'), \tag{21}$$

$$P_0(n) = \exp(-\beta'\epsilon - \gamma' n)/q_v(\beta', \gamma'), \tag{22}$$

where the new partition functions $Q(\beta', \gamma') = q_t(\beta')q_v(\beta', \gamma')$ ensure the normalization of probabilities. The Lagrange parameters β' and γ' are determined via

$$A = -\partial \ln Q(\beta', \gamma')/\partial\beta' = -\partial \ln q_t(\beta')/\partial\beta' - \partial \ln q_v(\beta', \gamma')/\partial\gamma', \tag{23}$$

$$B = -\partial \ln Q(\beta', \gamma')/\partial\gamma' = -\partial \ln q_v(\beta', \gamma')/\partial\gamma'. \tag{24}$$

It should be noted that since β' satisfy the two independent equations, (23) and (24), while β_0 satisfy the single equation (10), $\beta' \neq \beta_0$. The constant A has the same value in (10) and (23). If, accidentally $\beta' = \beta_0$ then (24) is a "non-informative", i.e. redundant constraint. This for example is the case when the levels are harmonic, $\epsilon_n = nh\omega$.

There is an additional important difference between the equilibrium solutions (20) and (8). While the latter is the stationary solution of the full master equation (4), the former corresponds to a modification of (4) in which the sum on the right hand side involves only v–v ($\langle n\rangle$ conserving) collisions, i.e. $n + m = n' + m'$. Setting again $a = \epsilon, n$ in (3), using (20) and noting that $\exp[-\gamma'(n + m - n' + m')] = 0$, we find that the detailed rate constants in the modified master equation satisfy (11); (as expected, since (11) is essentially the microscopic reversibility principle).

Assuming again that t/r relaxation is instantaneous we can employ (11) to integrate the modified master equation over ϵ, e, ϵ' and e' and get, cf. (13),

$$\mathrm{d}P(n)/\mathrm{d}t = -\rho \sum_{m,n',m'} \delta(n+m-n'-m')[k(n,m\to n',m';\beta)P(n)P(m) - k(n',m'\to n,m;\beta)P(n')P(m')] \;, \quad (25)$$

where the δ function ensures $\langle n \rangle$ conservation. Note that $\beta = \beta(t) \neq \beta'$ except at $t \to \infty$. From (11) and (12) it follows that the time dependent rate constants satisfy (15). (Setting $\mathrm{d}P(n)/\mathrm{d}t = 0$ in (25) we obtain the lowest order term in the Chapman–Enskog expansion of (13) in terms of $\tau_{\mathrm{vt}}/\tau_{\mathrm{vv}}$ [2].)

Finally, by direct substitution of the canonical-like distribution

$$P_{\mathrm{c}}(n) = \exp(-\beta\epsilon - \gamma n)/q_{\mathrm{v}}(\beta, \gamma), \quad (26)$$

it may appear that (26) is a stationary solution of (25) for each momentary value of β and regardless of the value of γ. To show that (26) is not an acceptable solution we may treat γ as time dependent. (This includes $\dot{\gamma} = 0$ as a special case.) As in the passage from (16) to (17), derivation of (26) yields

$$\dot{P}_{\mathrm{c}}(n) = -[(\epsilon_n - \langle \epsilon_n \rangle)\dot{\beta} + (n - \langle n \rangle)\dot{\gamma}]\, P_{\mathrm{c}}(n). \quad (27)$$

From this equation it is clear that $\dot{P}_{\mathrm{c}}(n) = 0$ only when both $\dot{\beta} = 0$ and $\dot{\gamma} = 0$. (The n dependence of the term in square brackets excludes the possibility that the terms with $\dot{\beta}$ and $\dot{\gamma}$ cancel out.) The resolution of the present "paradox" follows closely the lines of section 3. The major argument for rejecting (26) for finite t is that a stationary solution should satisfy, in addition to $\mathrm{d}P(n)/\mathrm{d}t = 0$, the rate equation for $\dot{\beta}$, (18). Alternatively, the only solution of the form (26) which satisfy both (23) and (24) is (20) for which $\beta = \beta'$ and $\gamma = \gamma'$.

In isothermal systems where $\beta = \beta_{\mathrm{b}}$ = const, the equilibrium (Treanor) distribution is given by (20) with β' replaced by β_{b} and γ' as evaluated from (24) with β_{b} instead of β'.

6. Concluding remarks

It was shown that thermodynamic considerations ensure the uniqueness of the detailed balance relation and the maximal entropy distribution as the only stationary solution of the master equation. It was emphasized that canonical-like distributions which by direct substitution into a reduced master equation may appear as stationary solution are quite often misleading because they are not consistent with the thermodynamic constraints. Particularly so, where only the reduced master equation for the slowly relaxing modes is considered.

Acknowledgement

We would like to thank Professor R.D. Levine for very helpful discussions.

References

[1] J.C. Light, J. Ross and K.E. Shuler, in: Kinetic processes in gases and plasmas, ed. A.R. Hochstim (Academic Press, New York, 1965).
[2] C.E. Treanor, J.W. Rich and R.G. Rehm, J. Chem. Phys. 48 (1968) 1798.
[3] R.D. Levine and A. Ben-Shaul, in: Chemical and biochemical applications of lasers, ed. C.B. Moore (Academic Press, New York, 1977).
[4] F. Reif, Statistical and thermal physics (McGraw-Hill, New York, 1965).

THE ROLE OF REAGENT INTERNAL EXCITATION IN COLLISION EXPERIMENTS*

A. Ben-Shaul and R.D. Levine
Department of Physical Chemistry
The Hebrew University, Jerusalem, Israel

Abstract

Variations in the rates of endoergic reactions due to different reagent excitations at the same total energy are of a limited (positive or negative) range and reflect a dynamical bias. Not so for bulk experiments where all nonselected degrees of freedom have a thermal distribution.

*Work supported by the Air Force Office of Scientific Research under Grants AFOSR 77-3135 and 77-3443.

1. Introduction

The role of reagent internal state in chemical reactions can be probed under two distinct types of conditions: (a) Single-collision experiments where not only the internal state but also the relative translational energy can be controlled [1-5] and (b) Bulk, macroscopic systems where typically all non-selected degrees of freedom have a thermal distribution [6-8]. The purpose of this letter is to contrast the results expected from these two types of experiments with special reference to endoergic reactions where experiments of type (b) will almost invariably lead to more dramatic enhancements of the reaction rate. It may indeed even be the case that at a given total energy, increasing the internal energy will decrease the reaction rate while the same change will significantly enhance the rate in an otherwise thermal experiment.

The different effects of reagent excitation in bulk and single collision experiments reflect two different aspects of the role of energy in chemical reactions. Changing the internal energy at a given total energy alters the dynamics of the collision. Such a change takes the collision through an entirely different region in phase space or, in a more classical language, corresponds to an entirely different set of reactive trajectories. On the other hand, the major effect of changing reagent internal excitation in an otherwise thermal experiment is, in the endothermic regime, to increase the fraction of molecules with energy in excess of the barrier [9-11]. There are, to be sure, dynamical effects also in bulk selection experiments, but the larger role is played by the purely thermochemical effect: In the

$$AB(n) + C \rightarrow AB + C \qquad (I)$$

reaction regard AB molecules of different internal levels as distinct chemical species, [11]. The endoergicity of the reaction from the ground state is ΔE_0.

The endoergicity for the reaction of AB(n) is $\Delta E_0 - E_n$. Increasing E_n is thus equivalent to a corresponding decrease in the endoergicity of the reaction.

Experimental results are more readily available on energy disposal in exoergic reactions, e.g. corresponding to (I)

$$A + BC \rightarrow AB(n) + C. \qquad \text{(II)}$$

Using detailed balance one can compare the dynamic bias of the forward and reverse reactions and show them to be the same, [10-13].

2. Detailed balance for single-collision experiments.

Consider the state-to-state diatom-atom endoergic reaction

$$AB(n) + C \rightarrow A + BC(n') \qquad \text{(III)}$$

at the total energy E. Here n and n' are labels of either single quantum states or of a group of degenerate states of AB and BC (e.g. the $g_J = 2J+1$ quantum states of a given v,J vibrotational level). Microscopic reversibility implies that [12-14]

$$g_n \rho_T(E-E_n) k(n \rightarrow n';E) = g_{n'} \rho_T'(E-\Delta E_0-E_{n'}) k(n' \rightarrow n;E) \qquad (1)$$

Here g_n is the degeneracy and $\rho_T(E_T)$ is the density of translational states, $\rho_T(E_T) = A_T E_T^{1/2}$ [9-13] at the translational energy E_T. The total energy E is measured in (1) from the ground state of AB+C. The energy of the ground state of A+BC then equals ΔE_0, the endoergicity.

Summing both sides of (1) over n' leads to the detailed balance relation for reaction (I)

$$g_n \rho_T(E-E_n) k(n\rightarrow;E) = \rho'(E) k(\rightarrow n;E) \qquad (2)$$

Here $k(\rightarrow n;E)$

$$k(\rightarrow n;E) = \sum_{n'} P^o(n'|E) k(n' \rightarrow n;E) \qquad (3)$$

$$P^o(n'|E) = g_{n'} \rho_T(E-\Delta E_0-E_{n'})/\rho'(E) \qquad (4)$$

$$\rho'(E) = \sum_{n'} g_{n'} \rho_T(E-\Delta E_0-E_{n'}) \qquad (5)$$

is the rate constant for the exoergic reaction (II) at the total energy E. The definition, (3), of $k(\rightarrow n;E)$ in terms of the state-to-state rates $k(n'\rightarrow n;E)$ is that implied by the canon, ('average over initial states'). $P^o(n|E)$ as defined by (4) and (5) is the prior distribution. $k(n\rightarrow;E)$,

$$k(n\rightarrow;E) = \sum_{n'} k(n\rightarrow n';E) \tag{6}$$

is the rate constant for the endoergic reaction (I), where the internal energy of AB is E_n and the relative translational energy of AB(n) and C is $E_T = E-E_n$. The definition (6) follows the canon, ('sum over final states'), and is valid whatever the energy distribution in the products A+BC of (II) may happen to be (except that their total energy is E).

The final form of (2) requires one more stage: Summing (2) over both n and n'

$$\rho(E)k(E) = \rho'(E)k'(E). \tag{7}$$

Here the two rate constants refer to the forward and reverse

$$A + BC \rightarrow AB + C \tag{IV}$$

reaction at the total energy E;

$$k'(E) = \sum_n k(\rightarrow n;E) \tag{8}$$

$$k(E) = \sum_n P^o(n|E)k(n\rightarrow;E) \tag{9}$$

$$P^o(n|E) = g_n\rho_T(E-E_n)/\rho(E) \tag{10}$$

$$\rho(E) = \sum_n g_n\rho_T(E-E_n). \tag{11}$$

Using (2), (7), (10) and (11) we obtain the rate constant from AB(n) at a total energy E, [12,15]

$$\begin{aligned} k(n\rightarrow;E) &= \rho'(E)k(\rightarrow n;E)/g_n\rho_T(E-E_n) = k(E)[P(n|E)/P^o(n|E)] \\ &\equiv k(E)\exp[-I(n|E)] \end{aligned} \tag{12}$$

Here $P(n|E)$ is the products' state distribution

$$P(n|E) = k(\rightarrow n;E)/k'(E) \tag{13}$$

in the exoergic A+BC reaction (II) at the total energy E. $P^o(n|E)$ as defined in (10) is the 'prior' distribution [13,16] of the products' states in the same reaction, and $I(n|E)$ is the surprisal.

The physical interpretation of (12) is immediate. Any dependence of $k(n\rightarrow;E)$, the rate constant of the AB(n)+C reaction, on the internal state of AB implies a dynamical bias in the energy disposal of the reversed A+BC reaction and vice-versa [11-13]. Hence, on prior grounds, i.e. in the absence of any dynamical bias, $(I(n|E)=0)$, all AB+C collisions with the same total energy have the same rate, irrespective of the partitioning of the energy between internal and translational degrees of freedom, [9].

We would like to emphasize that the result (12) is completely consistent with the conservation of angular momentum. Even such reactions where large changes in the reduced mass take place (e.g. Sr+HF → SrF+H, [1], or K+HCl → KCl+H, [2]) must still satisfy (12) with P^0 defined as in (10).

3. Lower resolution collision experiments.

Much of our knowledge about the role of internal energy in endoergic reactions derives, via detailed balance, from measurements of products' state distributions in the reversed, exoergic, processes. In many such experiments the resolution of products' internal states is limited to manifolds of states, α. The most obvious cases* being vibrational levels, $\alpha=v$, and translational energy shells, $(E_T, E_T+\Delta E_T)$, [12,16]. At a given total energy E, the detailed balance relation for the forward (endoergic) and reverse (exoergic) processes,

$$AB(\alpha) + C \rightleftarrows A + BC \qquad (V)$$

is obtained by summing both sides of (2) over the states n within the group α,

$$\rho(\alpha;E)k(\alpha\rightarrow;E) = \rho'(E)k(\rightarrow\alpha;E). \qquad (14)$$

---

[*] At a given E specifying v corresponds to many translational-rotational states with joint energy $E_T+E_J = E-E_v$. Similarly, there are usually many v,J states within the energy interval $E-(E_T+\Delta E_T) \leq E_{v,J} \leq E-E_T$.

Here

$$\rho(\alpha;E) = \sum_n{}' g_n \rho_T(E-E_n) \tag{15}$$

$$k(\alpha \to ;E) = \sum_n{}' P^o(n|\alpha) k(n \to ;E) \tag{16}$$

$$P^o(n|\alpha) = g_n \rho_T(E-E_n)/\rho(\alpha;E) \tag{17}$$

$$k(\to \alpha;E) = \sum_n{}' k(\to n;E) \tag{18}$$

where the prime over the summation signifies the restriction to states n in the group α. Using (14) and (7) we obtain, in analogy to (12)

$$k(\alpha \to ;E) = k(E)[P(\alpha|E)/P^o(\alpha|E)] \equiv k(E)\exp[-I(\alpha|E)] \tag{19}$$

where $P(\alpha|E)$ and $P^o(\alpha|E)$,

$$P(\alpha|E) = k(\to \alpha;E)/k'(E) \tag{20}$$

$$P^o(\alpha|E) = \rho(\alpha;E)/\rho(E) \tag{21}$$

are the products' 'α' distribution in the reverse reaction and the prior distribution, respectively. The relative rate $k(\alpha \to ;E)/k(E)$, like $k(n \to ;E)/k(E)$ cf. (12), depends on any reagent state preparation only if there is a dynamical bias., i.e. if the surprisal $I(\alpha|E) \neq 0$.

4. Example

The efficacy of different partitions of a given total energy between the different degrees of freedom of the reagents is determined by the surprisal. Enhancement occurs for such initial states whose surprisal is negative while a rate below the average corresponds to initial states of positive surprisal*. For endoergic reactions the magnitude of the surprisal can be determined from experimental (or computational) studies of energy disposal in the reversed

---

[*] By the canon, k(E) is the average rate constant,hence, unless all states react with the same rate, there must be states which react with a smaller than average rate. In other words, if some partitioning of the total energy enhances the rate then, necessarily, some other partitioning decreases the rate.

exoergic, reactions. The available results of such studies are that the surprisal is seldom larger than a couple of units. Hence the typical dynamical bias provided by nature suffices for at most about two orders of magnitude of variation in the relative rates (at a given total energy).

To emphasize the limited, albeit respectable range of reaction rates possible for different partitions of a given energy we consider the endoergic

$$H + HF(\alpha) \rightarrow H_2 + F \qquad (\Delta E_0 \approx 32 \text{ kcal/mole}) \qquad \text{(VI)}$$

reaction. The surprisal for the reversed reaction is well characterized [17-21], for thermal reactants. Due to the considerable exoergicity, the spread in the total energy in the products of the $F+H_2 \rightarrow H+HF$ reaction is small. Hence, to a good approximation the surprisal for H+HF is known at a given total energy ($\cong \Delta E_0 + (5/2)RT + E_a$, where E_a, the activation energy is about 1 kcal/mole, [22]).

Three choices of α will be considered:

i) $\alpha = v$. The vibrational surprisal for $E_v \leq \Delta E_0$ is quite linear

$$I(v|E) \equiv -\ell n[P(v|E)/P^o(v|E)] = \lambda_0 + \lambda_v f_v \qquad (22)$$

where $f_v = E_v/E$ and λ_v is a slowly decreasing function of E [20]. From (19) and (22)

$$k(v \rightarrow ;E)/k(v-1 \rightarrow ;E) = \exp(-\lambda_v \Delta f_v) \qquad (23)$$

where $\Delta f_v = f_v - f_{v-1} \approx 0.3$ for the H+HF(v) reaction at E just above ΔE_0. $\lambda_v \approx -6.9$, [17-20]. The enhancement of the rate by increasing HF internal excitation by a vibrational quantum ($\sim$ 11 kcal/mole) is less than an order of magnitude. By comparison, at 300 K, increasing the HF excitation by a vibrational quantum changes the rate by a factor of $\sim 10^9$ [10].

Similar conclusions obtain for the role of reagent vibration in other endoergic reactions. The recent report [1] that in the endoergic ($\Delta E_0 \approx 6$ kcal/mole) $Sr+HF \rightarrow SrF+H$ reaction at $E \approx 13$ kcal/mole, excitation of HF from v=0 to v=1 changed the rate by a factor of 1-10 is therefore consistent with our general expectations. The low enhancement factor is not necessarily indicative of the absence of a dynamical bias. Strict absence of bias requires that the ratio be unchanged and only a strong bias would provide a *factor of ten*.

ii) $\alpha = v,J$. The vibrotational surprisal for $F+H_2$ is well represented by

$$I(v,J|E) = \lambda_v f_v + \Theta_R f_R/(1-f_v) + \lambda_0 . \qquad (24)$$

Here $f_R = E_R/E$ is the fraction of the total energy in rotation. For $F+H_2$ $\Theta_R = 1.75$ corresponding to $\hat{g}_R = 0.21$ where $\hat{g}_R$ is the most probable value of $g_R = f_R/(1-f_v)$, [21]. The relative rates

$$k(v,J \rightarrow ;E)/k(E) = \exp[-\lambda_v f_v - \Theta_R g_R - \lambda_0], \qquad (25)$$

are shown as a contour plot in Fig. 1. The peak is in the vicinity of the $f_v \rightarrow 1$ apex and the contours decrease by a factor of 2. We are aware that the qualitative shape of our contours differs from what others could have expected. Fig. 1 also shows the more familiar disposal plot of $P(v,J|E)$.

iii) $\alpha = J$ at constant v. The effect of pure rotational excitation is reflected by the ratio

$$k(v,J \rightarrow ;E)/k(v,J-1 \rightarrow ;E) = \exp[-\Theta_R \Delta f_R/(1-f_v)] . \qquad (26)$$

Since typically $\Theta_R \gtrsim 0$, rotational excitation will usually decrease the reaction rate. The decline of the rate with increasing rotational state of HF is quite evident in Fig. 1. A qualitatively similar decline has recently been reported for the $K+HCl(v=1,J) \rightarrow KCl+H$ collision experiments, [2].

Exceptions to the unfavourable role of reagent rotation in collision experiments are possible for such rare cases that $\Theta_R < 0$. Examples are provided by reactions of OH(v,J), e.g. [23,24]

$$OH(v=0 \text{ or } 1,J) + NO \rightarrow H + NO_2 , \qquad (VII)$$

$$OH(v=0 \text{ or } 1,K) + H \rightarrow H_2 + O(^1D) . \qquad (VIII)$$

Contour plots showing the effects of changing reagent internal (or, equivalently, translational) excitation at a given E are available for the

$$M + CH_3I \rightarrow MI + CH_3 \qquad (IX)$$

reaction (M an alkali metal) [12], and similarly for [25]

$$K + RbF(CsF) \rightarrow KF + Rb(Cs) \qquad (X)$$

5. Thermal experiment

The detailed balance relation analogous to (12) for the case where nonselected degrees of freedom have a thermal distribution is [10,11]

$$k(\alpha \rightarrow ;T) = k(T)P(\alpha|T)/p(\alpha|T) \qquad (27)$$

$P(\alpha|T)$ is the distribution of $AB(\alpha)$ molecules in the thermal A+BC reaction. $p(\alpha|T)$ is the Boltzmann fraction of $AB(\alpha)$ molecules at the temperature T. *For a very* endoergic reaction, the reversed reaction is very exoergic and hence $P(\alpha|T) \gtrsim P(\alpha|E)$ at $E \cong \Delta E_0+E_a+(5/2)RT$. The essential differences between single collision experiments (19) and bulk experiments (27) is thus in the statistical factors $P^o(\alpha|E)$ vs. $p(\alpha|T)$. For exoergic reactions and when $E_\alpha \leq \Delta E_0$, $P^o(\alpha|E)$ is only a moderately varying function of α vs. the strong dependence of $p(\alpha|T)$ on E_α at lower temperatures. As the bulk temperature is increased, the differences between the two types of experiments will diminish.

In the Tolman interpretation [26], the activation energy is the difference between the mean energy of those molecules that react and the mean energy of all molecules. From (27)

$$E_a(\alpha) \equiv -RT^2\partial\ell nk(\alpha \rightarrow ;T)/\partial T = E_a-E_\alpha-RT^2\partial\ell nP(\alpha|T)/\partial T. \qquad (28)$$

Here E_a is the activation energy of the purely thermal reaction. $-E_\alpha \equiv RT^2\partial\ell np(\alpha|T)/\partial T$ is the change in energy of all molecules due to selective population of $AB(\alpha)$ while $E_a^\ddagger(\alpha)$,

$$E_a^\ddagger(\alpha) = -RT^2\partial\ell nP(\alpha|T)/\partial T \qquad (29)$$

is the change in the mean energy of those molecules that react. The empirical finding [9] that $E_a^\ddagger(\alpha)$, is smaller than E_α or roughly for $\alpha = v$,

$$E_a^\ddagger(v) \approx \lambda_v(RT/E)E_v \qquad (30)$$

where $-\lambda_v(RT/E)$ is typically below 0.25 implies that the primary (>75%) cause for the enhancement of the bulk rate is the increase in the mean energy of all molecules, while the reduction in the mean energy of those molecules that react is a secondary (<25%) effect.

Acknowledgement

We thank Drs. Y. Haas and K.L. Kompa for suggesting the need to clarify the differences between the role of reagent excitation in bulk and single-collision experiments.

References

1. A. Gupta, D.S. Perry and R.N. Zare, J. Chem. Phys. (in press).
2. H.H. Dispert, M.W. Geis and P.R. Brooks, J. Chem. Phys. 70 (1979) 5910.
3. A.M. Moutinho, A.W. Kleyn and J. Los, Chem. Phys. Letters 61 (1979) 249.
4. L. Zandee and R.B. Bernstein, J. Chem. Phys. 68 (1978) 3760.
5. K.G. Anlauf, D.H. Maylotte, J.C. Polanyi and R.B. Bernstein, J. Chem. Phys. 51 (1969) 5716; D.S. Perry, J.C. Polanyi and C.W. Wilson, Chem. Phys. Letters 24 (1974) 484; R.B. Bernstein and R.D. Levine, Adv. At. Mol. Phys. 11 (1975) 215.
6. D.J. Douglas, J.C. Polanyi and J.J. Sloan, Chem. Phys. 13 (1976) 15.
7. J. Wolfrum, Ber. Bunsenges. Phys. Chem. 81 (1977) 114.
8. A. Ben-Shaul, Y. Haas, K.L. Kompa and R.D. Levine, 'Lasers and Chemical Change' (Springer, Heidelberg, 1980).
9. R.D. Levine and J. Manz, J. Chem. Phys. 63 (1975) 4280.
10. H. Kaplan, R.D. Levine and J. Manz, Chem. Phys. 12 (1976) 447.
11. R.D. Levine in 'The New World of Quantum Chemistry'. B. Pullman and R. Parr eds. (Reidel, Dordrecht, 1976), p. 103.
12. H. Kaplan and R.D. Levine, Chem. Phys. 18 (1976) 103.
13. J.L. Kinsey and R.D. Levine, Chap. 22 in 'Atomic and Molecular Collision Theory', R.B. Bernstein ed. (Plenum, New York, 1979).
14. J.C. Light, J. Ross and K.E. Shuler in 'Kinetic Processes in Gases and Plasmas', A.R. Hochstim ed. (Academic Press, New York, 1965).
15. C. Rebick, R.D. Levine and R.B. Bernstein, J. Chem. Phys. 60 (1974) 4977.
16. R.D. Levine and A. Ben-Shaul, in 'Chemical and Biochemical Applications of Lasers', Vol. II, p. 145, C.B. Moore ed. (Academic Press, New York, 1977).
17. A. Ben-Shaul, R.D. Levine and R.B. Bernstein, J. Chem. Phys. 57 (1972) 5427.
18. M.J. Berry, J. Chem. Phys. 59 (1973) 6229.
19. D.S. Perry and J.C. Polanyi, Chem. Phys. 12 (1976) 419.
20. W.A. Wassam and R.D. Levine, Mol. Phys. 33 (1977) 689.
21. R.D. Levine, B.R. Johnson and R.B. Bernstein, Chem. Phys. Letters 19 (1973) 1.
22. E. Würzberg and P.L. Houston (to be published).

23. J.A. Silver, W.L. Dimpfl, J.H. Brophy and J.L. Kinsey, J. Chem. Phys. 65 (1976) 1811.
24. A.C. Luntz, R. Schinke, W.A. Lester and Hs. H. Günthard, J. Chem. Phys. 70 (1979) 5908.
25. M. Tamir and R.D. Levine, Chem. Phys. 18 (1976) 125.
26. R.D. Levine and R.B. Bernstein, Molecular Reaction Dynamics (Clarendon Press, Oxford, 1974).

Figure legend

1 a. Contour plot of $k(v,J \rightarrow ;E)/k(E)$ for the H+HF(v,J) reaction at $E \cong 34$ kcal/mole. Shown are contours connecting different partitionings of the total energy E which have the same reaction rate according to (25). $\lambda_v = -6.9$, $\theta_R = 1.75$. The highest contour is in the uppermost, $f_v \rightarrow 1$ apex and successive contours correspond to a decline of the rate by a factor of 2. The dashed contour is the one of zero surprisal. Partitions of the total energy which are in the region above it enhance the rate, while those which are below correspond to a rate below average.

b. Contour plot of the products' $P(v,J|E)$ distribution in the $F+H_2$ reaction. Note that the two plots are related by the detailed balance equation (19).

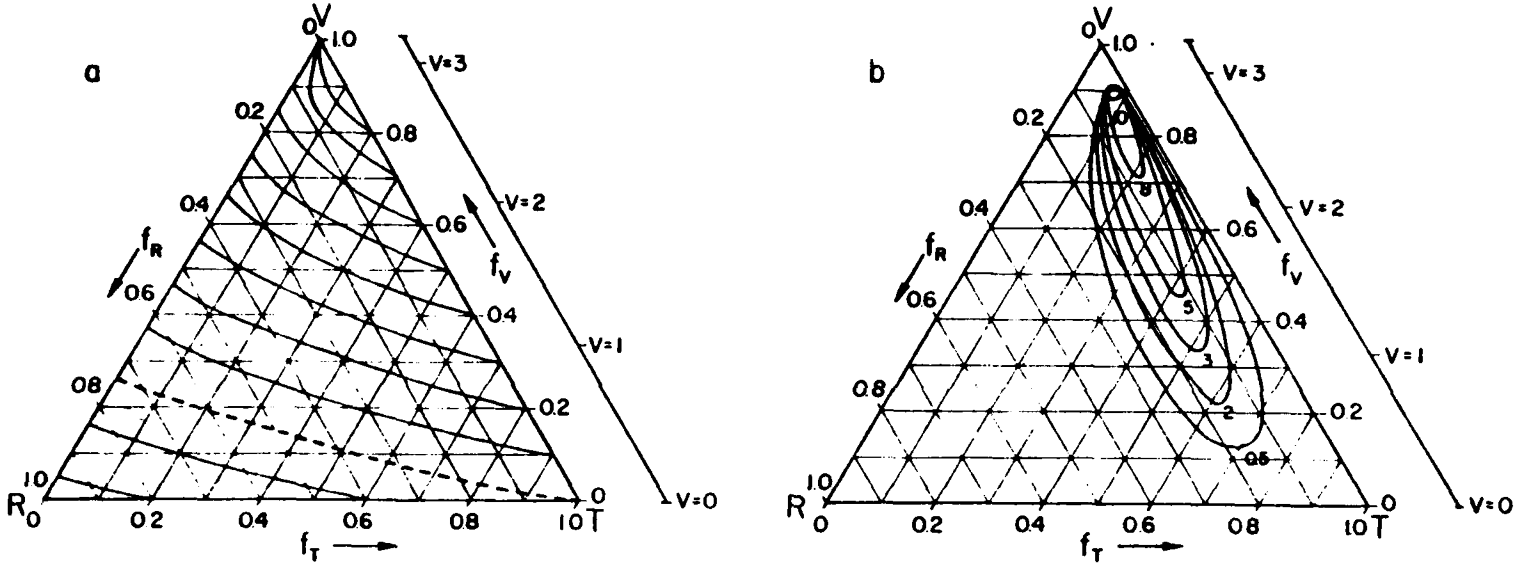

Figure 1

LASERS AND CHEMICAL CHANGE

A. Ben-Shaul, Y. Haas, K.L. Kompa and R.D. Levine

Springer Series in Chemical Physics
Springer Verlag, Berlin, Heidelberg, New York, 1980

Notice last page

LASERS AND CHEMICAL CHANGE

TABLE OF CONTENTS

Preface

Chapter 1. Lasers and Chemical Change

1.1 Light Amplification and Population Inversion in Chemical Processes

1.2 Molecular Rate Processes

1.3 Photoselective Chemistry

1.3.1 The Discrete Spectrum

1.3.2 The Quasicontinuum

1.3.3 Radiationless Transitions

1.3.4 Dissociative Continuum

1.3.5 Ionization

1.4 *The Road Ahead*

Chapter 2. Disequilibrium

2.1 Specificity and Selectivity of Chemical Reactions

2.1.1 Overview: Microscopic Disequilibrium

2.1.2 The Detailed Rate Constant

2.1.3 Detailed Balance

2.1.4 Energy Disposal and Energy Consumption

2.1.5 The Reaction Probability Matrix

2.1.6 Measures of Specificity and Selectivity

2.1.7 The Maximum Entropy Formalism

2.2 Surprisal Analysis

- 2.2.1 The Prior Distribution
- 2.2.2 The Surprisal
- 2.2.3 Vibrational Surprisal
- 2.2.4 Rotational Surprisal
- 2.2.5 Electronic Excitation
- 2.2.6 Polyatomic Molecules
- 2.2.7 Surprisal Analysis and Collision Dynamics
- 2.2.8 On the Role of Reagent Translation

2.3 Molecular Reaction Dynamics

- 2.3.1 Computational Studies
- 2.3.2 Potential Energy Surface(s)
- 2.3.3 Bond-Tightening Models
- 2.3.4 Kinematic Models of Collision Dynamics
- 2.3.5 Unimolecular Processes - the RRK Approach
- 2.3.6 Unimolecular Processes - Specificity and Selectivity
- 2.3.7 Preparing the Initial State

2.4 State to State Processes

- 2.4.1 The Prior Detailed Rate Constant
- 2.4.2 The Exponential Gap Representation
- 2.4.3 Reactive Collisions
- 2.4.4 The Adiabaticity Parameter
- 2.4.5 Polyatomic Molecules

2.4.6 Temperature Dependence

2.4.7 Electronic Energy Transfer

2.4.8 A Laser Bridge for the Exponential Gap

2.4.9 Intramolecular Electronic to Vibrational Energy Transfer: Radiationless Transitions

2.5 Macroscopic Disequilibrium

2.5.1 The Master Equation: Relaxation of Harmonic Oscillators

2.5.2 Rotational Relaxation

2.5.3 Separation of Time-Scales

2.5.4 Vibrational Anharmonicity and Up-pumping

2.5.5 Intermode V-V Transfer

2.5.6 Macroscopic Relaxation and Microscopic Information

2.5.7 Thermodynamics of Molecular Disequilibrium

2.5.8 Laser Thermodynamics

Appendices

2.A The Prior Distribution

2.B Practical Surprisal Analysis

2.C Statistical Mechanics of Molecular Collisions

2.D The Treanor Distribution

Chapter 3. Photons, Molecules and Lasers

3.1 Interaction of Molecules with Radiation
  3.1.1 The Golden Rule
  3.1.2 The Lineshape Function
  3.1.3 Coherent Interaction

3.2 Essential Physics of Lasers
  3.2.1 The Gain Coeffcient
  3.2.2 Laser Oscillations
  3.2.3 Laser Radiation and Modes
  3.2.4 The Laser Rate Equations

3.3 Survey of Atomic and Molecular Spectroscopy
  3.3.1 Atomic Spectra
  3.3.2 Molecular Spectra
  3.3.3 Electronic Spectra of Diatomic Molecules
  3.3.4 Infrared Spectrum of Diatomic Molecules
  3.3.5 Energy Levels of Polyatomic Molecules
  3.3.6 Infrared Spectrum of Polyatomic Molecules
  3.3.7 The Near Ultraviolet Spectrum of Carbonyl Compounds

3.4 Laser Sources
  3.4.1 Laser Specifications
  3.4.2 Exciplex Lasers
  3.4.3 Dye Lasers
  3.4.4 CO_2 Lasers

Chapter 4. Chemical Lasers

- 4.1 Survey of Chemical Lasers
- 4.2 Lasing Conditions in Chemical Lasers
- 4.3 Operation
  - 4.3.1 Flash Photolysis: The Iodine Laser as a Model Case
  - 4.3.2 Hydrogen Halide Chemical Lasers
  - 4.3.3 The Chemical CO Laser

- 4.4 Chemical Laser Kinetics
  - 4.4.1 The Rate Equations
  - 4.4.2 Rotational Equilibrium
  - 4.4.3 Rotational Nonequilibrium
  - 4.4.4 cw Chemical Lasers

- 4.5 Some Applications of Chemical Lasers
  - 4.5.1 Total Rate Constants, Kinetic Isotope Effects
  - 4.5.2 Vibrational Population Ratios From Threshold Measurements
  - 4.5.3 Gain Probing
  - 4.5.4 Energy Transfer Measurements: An Example
  - 4.5.5 An Industrial Diagnostic Application

Chapter 5. Laser Chemistry

5.1 The Laser Evolution

5.2 Bimolecular Reactions

- 5.2.1 Molecular Beam Studies
- 5.2.2 Reactions in the Bulk

5.3 Electronic Excitation of Polyatomic Molecules

- 5.3.1 Direct Photodissociation: The A state of ICN
- 5.3.2 Photopredissociation: Formaldehyde
- 5.3.3 Excitation of Bound Electronic States: Biacetyl and Glyoxal

5.4 Multiphoton Activation and Fragmentation

- 5.4.1 The Nature of Multiphoton Excitation
- 5.4.2 The Rate Equation Approach
- 5.4.3 Non-dissociative Reactions Induced by Multiphoton Absorptions
- 5.4.4 Multiphoton Ionization

5.5 The 'Compleat' Laser Chemist

- 5.5.1 The Practice of Laser Chemistry
- 5.5.2 Laser Based Diagnostic Techniques

5.6 From the Laboratory to Large Scale Laser Chemistry

- 5.6.1 Practical Photoselective Chemistry
- 5.6.2 State Selective Chemistry ?

Synergism

Preface

Lasers and chemical change is the study of radiation and molecules in disequilibrium. The distinguishing feature of such systems is the extreme departure from thermal equilibrium: the radiation is usually confined to a narrow frequency range, is well collimated and is far brighter than a black body radiation; the chemical composition and also the distribution of molecules over their different energy states is often markedly displaced from that expected at equilibrium. Such systems can be used as a source of laser radiation and, reversedly, lasers can rapidly and selectively displace molecular systems from equilibrium. The subsequent evolution of the initially prepared state can then be monitored - again using lasers.

One purpose of this book is to introduce the concepts required to discuss systems of radiation and molecules in disequilibrium. These include the physics of (laser) radiation and of radiation-matter interaction and molecular structure and spectroscopy. Excellent textbooks of these topics are available and our survey (in Chap. 3) is only intended to accent the essential points, with special reference to atomic and molecular radiation physics. Considerably more attention is given to the topic of disequilibrium in chemical systems (Chap. 2). In particular we consider both inter- and intra-molecular dynamics with special reference to energy requirements and energy disposal in chemical reactions and to what goes on in between - intramolecular energy migration. Disequilibrium in macroscopic systems and their temporal evolution is then discussed in terms of the underlying molecular events. The discussion throughout is in terms of a thermodynamic-like formulation motivated by information theoretic considerations and is illustrated by examples drawn from current studies. The principles of the design of such experiments, the experimental setups as used in practice and the nature and interpretation of typical results are discussed in detail in Chapters 4 and 5.

Lasers and chemical change is primarily the study of the phenomena of interconversion of radiant and chemical energy. Exoergic chemical reactions can be employed to generate laser radiation and lasers can be used to induce and to interrogate chemical reactions. The first chapter is an introduction of these two broad classes of phenomena (which are then treated in more detail in Chapters 4 and 5). It also serves to motivate the need for the theoretical concepts introduced in Chapters 2 and 3. The first chapter is self-contained, but many details are glossed over. The basic phenomena and the essential interpretation can however be found there.

to /

Large sections of chapters 4 and 5 are devoted to case studies. Attention is given to the experimental arrangements with special reference to the more commonly used techniques. Chapters 4 and 5 describe the practice of chemical lasers and laser induced chemistry, including the blending of experimental studies and theoretical interpretation.

The material in Chap. 1 is suitable for inclusion in advanced undergraduate physical chemistry courses. The other chapters are for the graduate level. It is however our intention and hope that they will also prove useful to the specialist. The selection of topics and their relative emphasis reflects not only our judgment but also our expertise and research interests, the overall progress in the field and the availability of other sources. In particular, laser induced processes in condensed phases (solutions, matrices, mixed crystals) and in biological systems are not covered. We have not tried to be exhaustive and the list of references is by no means complete and is only meant to offer an access to the literature. We have tried to offer an integrated picture, to emphasize chemical reactions and chemical lasers, to draw attention to the complexities and the promises associated with the use of larger molecules and to stress the theme of disequilibrium on both the microscopic and macroscopic levels.

The rapid progress in this field has been made possible by the elegant and probing experiments and the incisive interpretation carried out by many of our colleagues. Inspection of the contents of this volume demonstrates the magnitude of our debt to them. Our own work has been supported by the U.S. Air Force Office of Scientific Research, the Israel Academy of Sciences and Humanities, the Bundesministerium für Forschung und Technologie and the Max Planck Gesellschaft zur Förderung der Wissenschaften e.V.. We also wish to thank Dr. M.J. Berry for his involvement during the initial stages of this project and Dr. H.K.V. Lotsch of the Springer Verlag for his consistent advise ~~encouragement~~ and for not giving up / hope. Last but not least, we are very grateful to our families for their continuous encouragement and support.

A.B-S.
Y.H.
K.L.K.
R.D.L.

Department of Physical Chemistry
The Hebrew University
Jerusalem, Israel

and

Projektgruppe für Laserforschung
Max-Planck-Gesellschaft zur Förderung
der Wissenschaften e.V.
Garching, Germany

December, 1979
January 1980